Review

Recent Research Progress on All-Solid-State Mg Batteries

Jayaraman Pandeeswari , Gunamony Jenisha , Kumlachew Zelalem Walle , Masashi Kotobuki *

Posted Date: 10 October 2023

doi: 10.20944/preprints202310.0484.v1

Keywords: magnesium battery; solid electrolyte; ceramic electrolyte; polymer electrolyte; all-solid-state Mg battery

Review

Recent Research Progress on All-Solid-State Mg Batteries

Jayaraman Pandeeswari, Gunamony Jenisha, Kumlachew Zelalem Walle and Masashi Kotobuki *

Battery Research Center of Green Energy, Ming Chi University of Technology, 84 Gungjuan Rd., Taishan Dist., New Taipei City, 24301, Taiwan; pandeesj@gmail.com (J.P.); jenishagunamony@gamil.com (G.J.); kzeybelay1@gmail.com (K.Z.)

* Correspondence: kotobuki@mail.mcut.edu.tw

Abstract: Current Li battery technology employs graphite anode and flammable organic liquid electrolytes. Thus, current Li battery is always facing the problems of low energy density and safety. Additionally, sustainable supply of Li due to scarce abundance of Li sources is another problem. All-solid-state Mg battery is expected to solve the problems owing to non-flammable solid-state electrolytes, high capacity/safety of divalent Mg metal anode and high abundance of Mg sources. Therefore, solid-state electrolytes and all-solid-state Mg battery have been researched intensively last two decades. However, realization of all-solid-state Mg battery is still far. In this article, we review recent research progress on all-solid-state Mg battery so that researchers can pursue recent research trend of all-solid-state Mg battery. At first, solid-state electrolyte research is described briefly in the categories of inorganic, organic and inorganic/organic composite electrolytes. After that, the recent research progress of all-solid-state Mg battery is summarized and analyzed. To help readers, we tabulate electrode materials, experimental conditions and performances of all-solid-state Mg battery so that the readers can find necessary information at a glance. In the last, challenges to realize the all-solid-state Mg batteries are visited.

Keywords: magnesium battery; solid electrolyte; ceramic electrolyte; polymer electrolyte; all-solid-state Mg battery

1. Introduction

Since Li-ion battery (LIB) was commercialized in 1991, its application into portable electronic devices such as laptop computers and mobile phones has been widely achieved which has affected our daily life significantly [1,2]. As the most successful battery technology, LIBs possess several advantages including high energy density, no memory effect, good capacity retention, etc., overcoming last generation lead-acid and nickel hydrogen batteries [3,4]. Current LIBs rely on the intercalation mechanism. The energy density of LIBs has reached 240 Wh kg^{-1} and 670 Wh L^{-1} at the cell level due to the innovation and development of materials and cell design in these two decades [5,6]. However, the inherent limitation in the theoretical capacity of current graphite-based anodes makes LIBs be almost impossible to meet the increasing demand for energy density [7]. Li metal anode is an ideal anode material due to its ultimate high theoretical capacity (Table 1) which can improve the energy density of the batteries. Typically, Li-LMO cells (LMO means Li transition metal oxides) have revealed high energy density of ~ 440 Wh kg^{-1} [8]. However, dendric growth of Li metal and scarce abundance of Li source have hindered commercialization of the Li metal anode.

Solid-state electrolytes which are solid-state ion conductor can suppress the dendrite growth due to their high mechanical strength [9]. In addition, their inflammable nature and wide electrochemical window can improve the safety and energy density of LIBs. Therefore, solid-state electrolytes and all-solid-state Li batteries have been researched intensively especially in the last decade [10]. Regarding the low abundance of Li, it is considered that high abundance elements such as Na, K, Mg, Ca, Zn and Al are employed as a charge carrier instead of Li. Particularly, metal anodes

Preprints (www.preprints.org) | NOT PEER-REVIEWED | Posted: 10 October 2023 doi:10.20944/preprints202310.0484.v1

of multivalent ions (Mg^{2+}, Ca^{2+}, Zn^{2+}, Al^{3+}) possess higher volumetric capacities than monovalent Li metal anode. Table 1 summarizes representative properties of metal anodes. Mg has high abundance in the earth crust, high volumetric capacity and relatively low redox potential. Mg metal was believed to not form dendrite. Although the Mg dendrite formation was found in 2017 [11], less prone to dendrite formation of Mg metal comparing to Li and other metals is verified in both experimental and theoretical studies [12,13], making Mg metal be an ideal anode material. Therefore, research on all-solid-state Mg battery, Mg^{2+}-ion conductive solid-state electrolytes have been intensively carried out recently[14,15].

Solid-state electrolytes are categorized into three groups, organic, inorganic and organic-inorganic composite [16]. Typically, organic solid-state electrolytes are flexible and easy to process for large-scale production. Contrary, inorganic solid-state electrolytes commonly possess high ionic conductivity, high transference number, wide electrochemical window. The organic-inorganic solid-state electrolytes are proposed and developed to address the defects of organic and inorganic solid-state electrolytes which can combine the advantages of the flexibility and easy processing of organic solid-state electrolytes and high conductivity of inorganic solid-state electrolytes [17]. Some good review articles focusing on solid-state electrolytes have been published recently [18,19], while research on all-solid-state Mg batteries has yet to be reviewed.

Therefore, in this review article, we focus on recent, especially there five years (2018 ~), research on all-solid-state Mg battery. At first, solid-state electrolyte research is described briefly in the categories of inorganic, organic and inorganic-organic composite electrolytes. After that, the recent research progress of all-solid-state Mg battery is summarized and analyzed. To help readers, we tabulate electrode materials, experimental conditions and performances of all-solid-state Mg battery so that the readers can find necessary information at a glance. In the last, challenges to realize the all-solid-state Mg batteries are visited.

Table 1. Properties of various metal anodes.

	Li	Na	K	Mg	Ca	Zn	Al
Standard redox potential (E vs. SHE)	-3.04	-2.71	-2.93	-2.37	-2.87	-0.76	-1.66
Volumetric capacity (mAh/cm^3)	2062	1128	591	3883	2073	5851	8046
Specific capacity (mAh/g)	3861	1166	685	2205	1337	820	2980
Abundance (%)	0.002	2.7	2.4	2.08	5	0.008	8.2
Ionic radius (Å)	0.76	1.02	1.38	0.72	1.00	0.74	0.535
Relative atomic mass	6.94	22.98	39.1	24.31	40.08	65.39	26.98
Mass to charge	6.94	22.98	39.1	12.16	20.04	32.7	8.99

2. Solid electrolytes for Mg battery

2.1. Inorganic electrolyte

2.1.1. Oxides

Na^+ super ion conductor (NASICON), $Na_{1+x}Zr_2P_{3-x}Si_xO_{12}$ is well-known for permitting fast migration of Na^+ ion due to the well-ordered three-dimensional network structure [20,21]. By the successful application of NASICON structure to Li+ ion conductive ceramic electrolyte such as $LiZr_2(PO_4)_3$ [22,23], $Li_{1+x}Al_xTi_{2-x}(PO_4)_3$ [24,25], and $Li_{1+x}Al_xGe_{2-x}(PO_4)_3$ [26,27], it has been highly interested in developing NASICON-type multivalent ion conductors [28,29].

Preprints (www.preprints.org) | NOT PEER-REVIEWED | Posted: 10 October 2023 doi:10.20944/preprints202310.0484.v1

The first report on NASICON-type Mg^{2+} ion conductors was $MgZr_4(PO_4)_6$ (MZP) in 1987 [30]. The ionic conductivity was 2.9×10^{-5} and 6.1×10^{-3} S cm^{-1} at 400 and 800 °C, respectively. MZP was assigned as the rhombohedral structure at first, but later it was ascribed to the monoclinic structure, which is like β-Fe_2SO_4. Nakayama et. al. simulated Mg^{2+} migration energy of 0.63 and 0.71 eV in the rhombohedral and monoclinic structures, respectively [31]. Thus, heteroatom doping into Zr^{4+} site to stabilize the rhombohedral structure has been carried out [32,33]. Contrary, another strategy, introduction of Hf^{4+} into Mg^{2+} site has also been attempted [34]. However, all results exhibited too low Mg^{2+} ion conductivity, ~ 10^{-5} S cm^{-1} even at 500 °C. Those cannot be applied for all-solid-state Mg battery operated at ambient temperature. It is noted that some promising results were reported by Mohamed's group. They reported $\sigma = 3.97 \times 10^{-4}$ S cm^{-1} at room temperature in $Mg_{1.05}Zn_{0.4}Al_{0.3}Zr_{1.3}(PO_4)_3$. However, this material demonstrated almost the same conductivity, 5.82×10^{-4} S cm^{-1} at 500 °C [35]. The extremely low activation energy of 0.039 eV was about one order of magnitude lower than that of typical Li^+ ion conductive ceramics. They also estimated Mg^{2+} ion transference number by the Bruce method to 0.84 [33]. This implies 16 % of electric charge is carried by anion, i.e. oxygen ion. In addition, they measured electrochemical window of $Mg_{0.5}Si_2(PO_4)_3$ to 3.21 V, however, as shown in Figure 1, it seems decomposition of electrolyte commences below 2 V [36]. These data are quite weird. We need to re-check their results.

In other research, although magnesium phosphate ($Mg_{2.4}P_2O_{5.4}$) [37], magnesium silicate ($Mg_{0.6}Al_{1.2}Si_{1.8}O_6$) [38], magnesium tangstate ($MgHf(WO_4)_3$) [39] are researched, still a significant improvement of conductivity is needed. Indeed, all-solid-state Mg batteries using oxide-based solid electrolyte have not been reported yet.

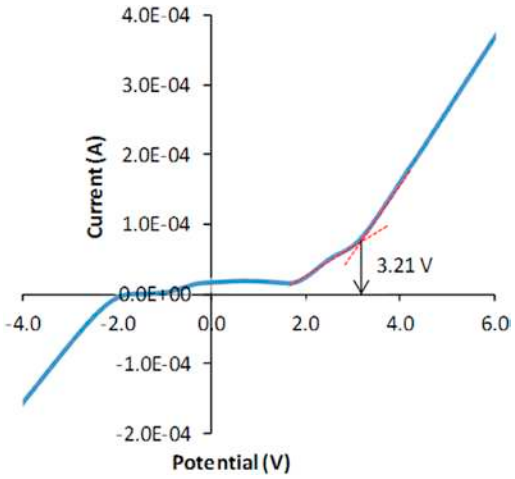

Figure 1. Linear sweep voltammogram of $Mg_{0.5}Si_2(PO_4)_3$. Reproduced with permission [36]. Copyright 2016, Elsevier.

2.1.2. Chalcogenides

Although chalcogenide-based Li^+ ion conductive ceramics like sulfides have succeeded greatly [40], chalcogenide-based Mg^{2+} ion conductive ceramics were not researched intensively. Only one paper was published about MgS-P_2S_5 system in 2014 [41]. However, since Canepa et. al. reported trinary spinel chalcogenides with high Mg^{2+} ion mobility in 2017 [42], research on the chalcogenide-based Mg^{2+} ion conductive ceramics has been activated. They predicted the least migration energy of Mg^{2+} ion appeared in MgY_2S_4, MgY_2Se_4 and $MgSc_2Se_4$ and the values were 360, 361 and 375 meV, respectively (Figure 2). However, only $MgSc_2Se_4$ has been successfully synthesized so far. The Mg^{2+} ion conductivity of $MgSc_2Se_4$ was estimated to ~ 1×10^{-4} S cm^{-1}, comparable to Li^+ ion conductive ceramic electrolytes (garnet-type and NASICON-type) [43]. Unfortunately, electronic conductivity was also relatively high about 4×10^{-8} S cm^{-1}. Thus, Fichtner et. al. synthesized Se-excess, Ti^{4+}, Ce^{4+}-doped $MgSc_2Se_4$ to reduce the electronic conductivity, but the electronic conductivity was not drastically lowered [44]. Based on this, they used $MgSc_2Se_4$ as a cathode material for Mg battery using liquid electrolyte. Kundo et. al. studied electronic conduction mechanism of $MgSc_2Se_4$ and found

Preprints (www.preprints.org) | NOT PEER-REVIEWED | Posted: 10 October 2023 doi:10.20944/preprints202310.0484.v1

electronic conductive layer was formed on the surface of particles during ball-milling process [45]. In fact, the electronic conductivity was reduced by avoiding ball-milling process. In addition, the ionic and electronic conductivities of $MgSc_2Se_4$ were largely influenced by sintering process, particularly cooling process. Indeed, the field-assisted synthesis could sinter $MgSc_2Se_4$ in very short time, leading to low electronic conductivity of $\approx 10^{-11}$ S cm^{-1} [46]. Lowering the electronic conductivity of $MgSc_2Se_4$ is a critical issue to apply for all-solid-state Mg batteries. Advanced sintering techniques which can provide rapid heating/cooling rates and short heat treatment, such as spark plasma sintering (SPS) [23], flash sintering [47], microwave sintering [48] and ultrafast high temperature sintering [49] should be applied for sintering $MgSc_2Se_4$.

Electrochemical window of $MgSc_2Se_4$ has not been studied yet, but Au/$MgSc_2Se_4$/Au cell was stable during 3 V of applied voltage [46]. Therefore, $MgSc_2Se_4$ would possess reasonable electrochemical window for all-solid-state Mg battery application.

The development of $MgSc_2Se_4$ has two directions, electrolytes and electrodes. The electronic conductivity of $MgSc_2Se_4$ must be lowered for electrolytes while it is maintained for electrodes. The all-solid-state Mg battery composed of $MgSc_2Se_4$-based electrode and $MgSc_2Se_4$-based electrolyte should have an intimate electrode/electrolyte interface due to similar chemical composition and structure, resulting in high and stable performances.

Properties of oxide- and chalcogenide-based electrolytes are summarized in Table 2.

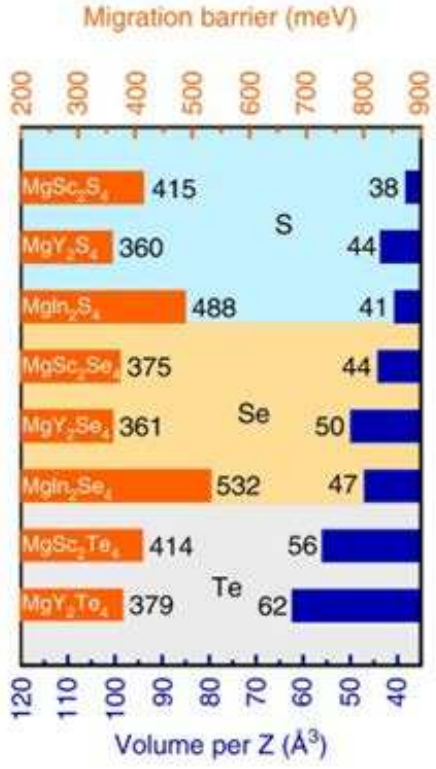

Figure 2. Computed Mg^{2+} ion migration barrier in trinary spinel chalcogenides. Reproduced with permission [42]. Copyright 2017, Nature Communications.

Table 2. Properties of various oxide- and chalcogenide-based solid electrolytes.

Electrolyte	σ_{total} (S cm^{-}	Temperature (^{o}C)	Activation energy (eV)	Electrochemical window (V)	Ref
Oxides					
$MgZr_4(PO_4)_6$	2.9	400	0.868	-	[30]
	6.1	800			
$Mg_{0.5}Zr_2(PO_4)_3$	1.1	30	0.0977	~ 2.5	[50]

Preprints (www.preprints.org) | NOT PEER-REVIEWED | Posted: 10 October 2023 doi:10.20944/preprints202310.0484.v1

	7.1	500			
$MgZr_4(PO_4)_6$	7.23	725	0.84	-	[51]
$MgZr_4(PO_4)_6$+$Zr_2O(PO_4)_2$	6.9	800	1.41	-	[52]
$Mg_{0.7}(Zr_{0.85}Nb_{0.15})_4(PO_4)_6$	5.71	800	0.95	-	[32]
$Mg_{1.4}Zr_4P_6O_{24.4}$+0.4$Zr_2O(PO_4)_2$	6.89	800	1.41	-	
$Mg_{1.1}(Zr_{0.85}Nb_{0.15})_4P_6O_{24}$+0.4$Zr_2O(PO_4)_2$	9.53	800	1.28	-	
$Mg_{1.1}Zr_{3.4}Nb_{0.6}P_6O_{24.4}$ + $Zr_2O(PO_4)_2$	9.53	800	1.26	-	[53]
$Mg_{0.9}Zr_{1.2}Fe_{0.8}(PO_4)_3$	1.25	RT	0.14	-	[33]
	7.2	500			
$Mg_{0.5}Ce_{0.2}Zr_{1.8}(PO_4)_3$	3.8	200	0.307	-	[54]
$Mg_{1.05}Zn_{0.4}Al_{0.3}Zr_{1.3}(PO_4)_3$	3.97	RT	0.039	-	[35]
	5.82	500			
$Mg_{0.35}(Zr_{0.85}Nb_{0.15})_2(PO_4)_3$	1.1	350	1.18	-	[55]
$Mg_{0.5}ZrSn(PO_4)_3$	2.47	500	0.79	-	[56]
$Mg_{0.7}Zr_{3.4}Nb_{0.6}(PO_4)_6$	7.7	600	0.954	-	[57]
	3.7	750			
$Mg_{0.6}Zr_{1.8}Fe_{0.2}(PO_4)_3$ thin film	1.8	25	0.141 < 175°C	-	[58]
	2.3	200			
$Mg_{0.625}Si_{1.75}Al_{0.25}(PO_4)_3$	1.54	RT	-	2.51	[59]
$Mg_{0.5}Si_2(PO_4)_3$	1.83	-		~ 3.21	[36]
$Mg_{0.105}Hf_{0.95}Nb(PO_4)_3$	1.2	600	0.639	-	[34]
$Mg_{2.4}P_2O_{5.4}$ ALD	1.6	500	1.37	-	[37]
$Mg_{0.6}Al_{1.2}Si_{1.8}O_6$	2.3	500	1.32	-	[38]
$MgSO_4$-$Mg(NO_3)_2$-MgO	2.2	RT	0.17	-	[60]
$MgHf(WO_4)_3$	2.5	600	0.835	-	[39]
Chalcogenides					
80(0.6MgS 0.4P_2S_5) 20MgI_2	2.1	200	-	-	[41]
$MgSc_2Se_4$	9.2	RT	-	-	[44]
$MgSc_2Se_4$	~1 ×	25	0.38		[42]
$MgSc_2Se_4$	8 ×	RT	-	-	[45]
$MgSc_2Se_4$	1.78	RT	-	-	[46]

2.1.3. Hydrides

In 2012, Matsuo et. al. reported possible Mg conduction in $Mg(BH_4)_2$ based on FPMD simulation [61]. Later, Higashi et. al. experimentally proved Mg ion conduction of $Mg(BH_4)_2$ and $Mg(BH_4)(NH_2)$ [62]. Since then, $Mg(BH_4)_2$-based electrolytes have been researched the most intensively among the inorganic solid electrolytes. Also, all-solid-state Mg battery with inorganic electrolytes has been fabricated by using only $Mg(BH_4)_2$-based electrolytes (Chapter 3.1). Although the ionic conductivity of $Mg(BH_4)(NH_2)$ is 1×10^{-6} S cm^{-1} at 150 °C [62], it is influenced by the synthetic parameter, for example, the ionic conductivity of 3×10^{-6} S cm^{-1} at 100 °C was obtained in glass-ceramic like $Mg(NH_4)(NH_2)$ [63]. As other strategies, modification of BH_4 ligands [64,65], partial oxidation [66],

Preprints (www.preprints.org) | NOT PEER-REVIEWED | Posted: 10 October 2023 doi:10.20944/preprints202310.0484.v1

compositing with ceramic oxides such as MgO, YSZ, TiO_2 and Al_2O_3 [67-70] have been attempted and all achieved improvement of Mg ion conductivity to 10^{-5} ~ 10^{-6} S cm^{-1} at ambient temperature which is slightly lower than those of Li and Na ion conductive inorganic solid electrolytes [10]. Additionally, they exhibited stable Mg plating/stripping behavior (Figure 3). However, the modification narrowed the electrochemical window to about 1.2 ~ 1.4 V. This restricts the choice of cathode materials and decreases the energy density of all-solid-state Mg batteries. Although the moderate ionic conductivity and stability against Mg metal anode of $Mg(BH_4)(NH_2)$-based inorganic solid electrolytes are desirable, improvement of anodic stability must be considered.

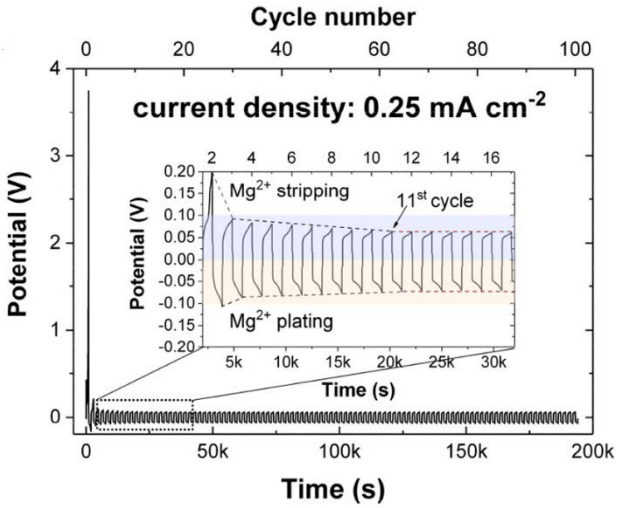

Figure 3. Galvanostatic cycling of a symmetric Mg/$Mg(BH_4)_2$ 1.6NH_3-MgO cell at 60 °C with a constant current density of 0.25 mA cm^{-2}. Reproduced with permission [69]. Copyright 2020, American Chemical Society.

Table 3. Properties of hydride-based solid electrolytes.

Electrolyte	σ_{total} (S cm^{-1})	Temperature (°C)	Activation energy (eV)	Electrochemical window (V)	Ref
$Mg(BH_4)_2$	1×10^{-9}	150	-	-	[62]
$Mg(BH_4)(NH_2)$	1×10^{-6}	150	-	3	
$Mg(en)_1(BH_4)_2$	5×10^{-8}	30	1.6	1.2	[64]
	6×10^{-5}	70			
$Mg(BH_4)(NH_2)$ glass	3×10^{-6}	100	1.3	-	[71]
$Mg(BH_4)_2$ 1.6NH_3-75 wt.%	1.2×10^{-5}	RT	1.12	1.2	[69]
Oxidized $Mg(BH_4)_2$	7.89 ×	RT	-	-	[66]
$Mg(BH_4)_2$ 1.5THF-75 wt.% MgO	9.8×10^{-7}	30	1.4	1.2	[70]
	1.7×10^{-4}	70			
$Mg(BH_4)_2(NH_3BH_3)_2$	1.3×10^{-5}	30	1.47	1.2	[65]
$Mg_3(BH_4)_4(NH_2)_2$	4.1×10^{-5}	100	0.84	1.48	[72]
Amorphous $Mg(BH_4)_2$ 2NH_3	5×10^{-4}	75	1.99	1.4	[73]
$Mg(BH_4)_2$ 1.5NH_3-60wt.%	3×10^{-4}	50	-	1.3	[67]
$Mg(BH_4)_2$ 1.5NH_3-60wt.%	1.12 ×	50	0.87	-	
$Mg(BH_4)_2$ 1.6NH_3-67 wt.%	2.5×10^{-5}	22	0.56	1.2	[68]

2.1.4. MOF (Metal-organic framework)

Preprints (www.preprints.org) | NOT PEER-REVIEWED | Posted: 10 October 2023 doi:10.20944/preprints202310.0484.v1

MOFs are crystalline solids composed of metal ions coordinated by multifunctional organic molecules with a three-dimensional porous structure. The composition and structure of MOFs can be easily adjusted via the rational selection of the metal ion and organic molecules [74]. Due to the porous structure, diffusivities of guest ions in the pores would be similar to those in molten salt state [75]. Therefore, MOFs have been studied as ionic conductors. To introduce guest ions, pores of MOFs are filled with liquid electrolytes. Thus, MOF-based solid electrolytes would be categorized into liquid-solid composite electrolyte.

Comparing to MOF-based Li^+ ion conductive electrolyte, the study for Mg^{2+} ion conductor is still few, only 8 papers have been published so far. The conductivity of MOF-based Mg ion conductive electrolytes ranges from 10^{-4} ~ 10^{-6} S cm^{-1}. Since MOF-based solid electrolytes contain liquid electrolytes, the transference number of Mg^{2+} ion should be studied as well as their electrochemical window. Only three papers reported those, 0.25 ~ 0.49 of transference number and about 3 V vs. Mg/Mg^{2+} of oxidative stability [76-78]. Contrary, stable Mg plating/stripping behavior was observed in 4 papers (Figure 4) [76-79]. Therefore, Mg metal anode can be applied for the MOF-based electrolytes. Typically, MOF-based Mg ion conductive electrolytes contain around 45 ~ 55 wt.% of solvent which is comparable to gel-polymer electrolytes [80], however, their conductivities and mechanical properties are not inversely proportional. Hassen et. al. reduced the liquid content in MOFs to around 20 wt.% and reported ionic conductivity was not primarily affected [76]. Also, the same group found conductivity enhancement by treatment of MOF at 150 °C for 24 h due probably to removal coordinated water.

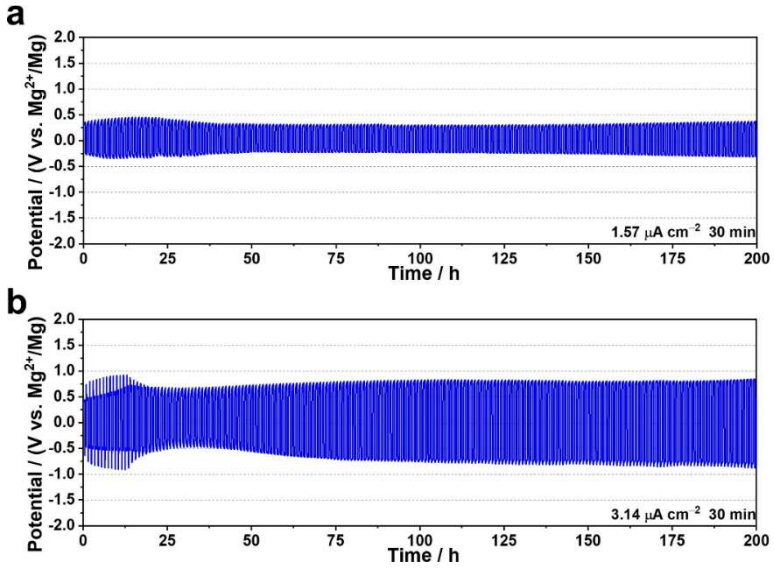

Figure 4. Mg plating/stripping test of UiO-66-$Mg(TFSI)_2$/[EMIM][TFSI] electrolyte at current density of (a) 1.57 μA cm^{-2} and (b) 3.14 μA cm^{-2} at 60 °C. Reproduced with permission [77]. Copyright 2022, Wiley-VCH GmbH.

The MOF-based electrolytes are likely to be stable for Mg metal anode, relatively high anodic stability, ~ 3 V and high conductivity which makes them a good candidate for all-solid-state Mg batteries. However, there are still a lot of unknowns. Particularly, the correlation of pore structure and composition of liquid electrolyte (salt, solvent, and salt concentration) with chemical/electrochemical properties must be clarified.

Table 4. Properties of MOF-based solid electrolytes.

MOF	Liquid electrolyte	σ_{total} (S cm^{-1})	Temperature (°C)	Activation energy (eV)	Ref
Mg_2(dobpdc)	$Mg(TFSI)_2$/triglyme	1.3×10^{-4}	RT	0.11 ~ 0.19	[80]
	$Mg(OPhCF_3)_2$+$Mg(TFSI)_2$/trigly	2.5×10^{-4}	RT		

Preprints (www.preprints.org) | NOT PEER-REVIEWED | Posted: 10 October 2023 doi:10.20944/preprints202310.0484.v1

MIT-20	$MgBr_2$/PC	8.8×10^{-7}	RT	0.37	[81]
$Cu_4(ttpm)_2$•0.6$CuCl_2$	$MgCl_2$/THF	1.2×10^{-5}	RT	0.32	[82]
	$MgBr_2$/THF	1.3×10^{-4}	RT	0.24	
MOF-74	$Mg(TFSI)_2/MgCl_2$/DME	3.17×10^{-6}	RT	0.53	[79]
Mgbp3dc	α-$Mg_3(HCOO)_6$/DMF	3.8×10^{-5}	RT	0.669	[76]
UiO-66	$Mg(TFSI)_2$/[EMIM][TFSI]	5.8×10^{-5}	RT	0.67	[77]
MOF-177	$Mg(TFSI)_2$/diglyme	1.6×10^{-5}	RT	0.33	[78]
MIL-101	$Mg(TFSI)_2$ + MeCN vapor	1.9×10^{-3}	25	0.18	[83]

2.2. Organic electrolyte

Organic electrolytes, that is, polymer electrolytes, are composed of polymer hosts and Mg salts (solid polymer electrolytes, SPEs). In some cases, fillers and plasticizers are added to improve the properties. SPEs have been reported the most, while SPEs with plasticizers are most widely employed for all-solid-state Mg batteries. Herein, recent research on organic electrolytes is briefly summarized. Recently, novel organic electrolytes, i.e., organic crystal electrolytes, are developed. Organic crystal electrolytes are introduced at the end of this section. For Mg^{2+} ion conductive electrolytes, only inorganic fillers are employed. Therefore, filler-added polymer electrolytes are reviewed in the next section "2.3 Organic-inorganic composite electrolytes".

2.2.1. Solid polymer electrolytes

SPEs are composed of host polymers and Mg salts. The Lewis-base moieties of host polymers allow the dissociation of Mg salts, resulting in emerging Mg^{2+} ion conduction. Accordingly, the host polymers contain atoms with lone-pair electrons such as oxygen, fluorine, and nitrogen atoms. Figure 5 depicts the structures of various host polymers.

Common host polymers such as PEO have been used in Mg^{2+}-ion conductive SPEs [84,85]. Different from Li^+ ion conductive SPEs, water-soluble polymers like PVP and PVA are also used [86-89]. Such polymers allow using water as a solvent, facilitating preparation processes and reducing production costs. The ionic conductivities of SPEs using the water-soluble polymer hosts are comparable (10^{-5} ~ 10^{-6} S cm^{-1}) to the conventional polymer hosts. However, other properties like the electrochemical window are seldom studied. Studies on the other properties must be carried out to clarify the applicability of the water-soluble polymer hosts.

Natural polymers are also used as host polymers for Mg^{2+} ion conductive SPEs [94-109]. Natural polymers are attractive in terms of environmental friendliness and resource abundance. Natural polymer-based SPEs exhibit better conductivity, around one order of magnitude higher than synthetic polymer-based SPEs. Notably, SPEs composed of potato starch and Gellan gum reveal high ionic conductivity of ~10^{-2} S cm^{-1} [97] which is comparable to $Li_{10}GeP_2S_{12}$ and even liquid electrolytes [110]. In addition, these SPEs possess high flexibility and are promising for all-solid-state Mg batteries. However, their application to all-solid-state Mg batteries has yet to be reported. The environmental friendliness of natural polymer means the natural polymers will decompose naturally in long-term. Thus, the long-term stability of natural polymer-based SPEs must be tested.

To improve the properties of SPEs, a polymer blend, that is, a mixture of two host polymers, is also studied [111-121]. By the blending, the ionic conductivity increases by one order of magnitude, 10^{-3} ~ 10^{-4} S cm^{-1}, which is applicable to all-solid-state Mg batteries. Recently, the blend of natural and synthetic polymers emerges as a new research trend in SPEs [122-125]. For example, in the blend of methyl cellulose (MC) and PVA, the hydrogen bond forms between MC and PVA, stabilizing the polymer blend [124]. In addition, rich-oxygen atoms in MC facilitate the dissociation of Mg salts. As a result, the ionic conductivity increased to ~ 10^{-4} S cm^{-1} which is applicable to all-solid-state Mg batteries [126].

Preprints (www.preprints.org) | NOT PEER-REVIEWED | Posted: 10 October 2023 doi:10.20944/preprints202310.0484.v1

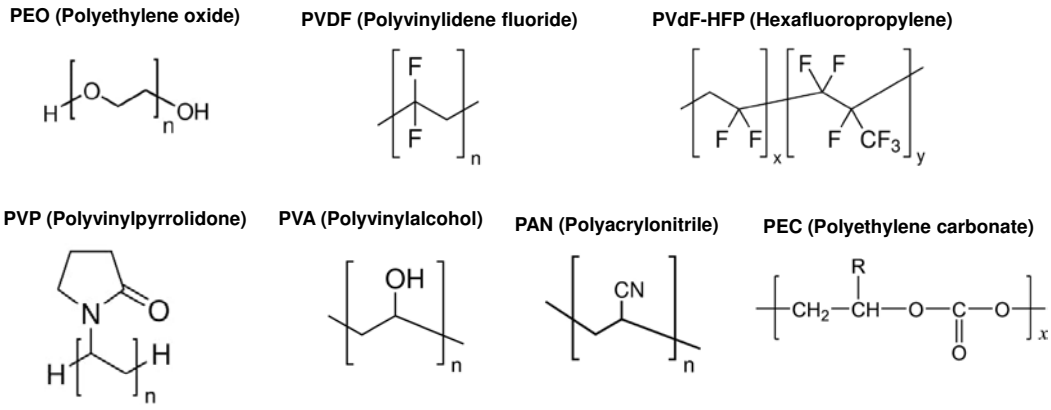

Figure 5. Structures of various host polymers used in Mg^{2+} ion conductive polymer electrolytes.

Regarding the Mg salts, in addition to commonly used metal salts in LIBs like TFSI, ClO_4-salts, more cost-effective $MgSO_4$, $Mg(NO_3)_2$, $MgCl_2$, etc. are used. Thus, water-soluble polymers such as PVA and PVP are used for these salts. The ionic conductivity was not influenced by the Mg salts. Aziz et. al. added LiFSI into PEC-$Mg(TFSI)_2$ SPE [92]. The ionic conductivity was improved by one order of magnitude by the addition. Also, the Li-contained SPE demonstrated stable Mg stripping and plating. The usage of mixing salt is a new concept for the SPEs. In this system, contribution of Li-ion conduction must be considered to estimate the ionic conductivity. However, characterization techniques to extract only Mg^{2+} ion conduction has not been developed yet. Therefore, characterization of the system should be paid extra consideration.

Many types of polymers and Mg salts are studied for Mg^{2+}-ion conductive SPEs. Most studies focus on the ionic conductivity, however, other properties such as electrochemical window, transference number and compatibility with electrodes are also important for application of all-solid-state batteries. Thus, studies on SPEs should be performed more comprehensively.

Table 5. Properties of SPEs.

Polymer	Mg salt	σ_{total} (S cm^{-1})	Temp.(°C)	E_a (eV)	Window (V vs. Mg/Mg^{2+})	Transference number	Ref
PEO	$Mg(TFSI)_2$	$1.8 \times 10^{-}$	0	0.68	-	-	[84]
		$1.6 \times 10^{-}$	50				
PEO	$Mg(ClO_4$	1.42 ×	RT	-	-	-	[85]
PVP	$MgCl_2$	1.42 ×	RT	-	-	-	[86]
PVP	$MgSO_4$	1.05 ×	RT	-	-	-	[87]
PVA	$MgSO_4$	1×10^{-9}	27	0.37	-	-	[88]
PVA	$MgCl_2$	5×10^{-7}	35	-	-	-	[89]
Polysaccharide	$Mg(ClO_4$	5.66 ×	RT	0.09	3.93	0.43	[90]
PEC	$Mg(ClO_4$	$5.2 \times 10^{-}$	90	-	-	-	[91]
PEC	Mg(TFSI	$2.3 \times 10^{-}$	80	-	2.0	-	[92]
PAGE	Mg(TFSI	$4.1 \times 10^{-}$	90	-	-	-	[93]
Potato starch	$MgCl_2$	$3.2 \times 10^{-}$	RT	0.002	4.6	-	[94]
Sodium	$Mg(NO_3$	4.58 ×	RT	-	3.5	0.31	[95]
MC	$Mg(NO_3$	1.02 ×	RT	-	3.23	-	[96]
Gellan gum	$Mg(ClO_4$	1.06 ×	RT	-	2.86	0.33	[97]

Preprints (www.preprints.org) | NOT PEER-REVIEWED | Posted: 10 October 2023 doi:10.20944/preprints202310.0484.v1

Natural rubber	$Mg(Tf)_2$	$4.9 \times 10^{-}$	30	-	2.5	-	[98]
I-	$Mg(NO_3$	$6.1 \times 10^{-}$	30	0.17	-	-	[99]
Agarose	$Mg(NO_3$	1.48 ×	RT	0.044	3.57	-	[100
CA	$Mg(NO_3$	9.19 ×	RT	-	3.65	0.35	[101
K-Carrageenan	$MgCl_2$	4.76 ×	30	-	1.94	0.26	[102
Chitosan	$Mg(Tf)_2$	9.58 ×	RT	0.36	-	-	[103
K-Carrageenan	$Mg(NO_3$	7.05 ×	RT	-	4.42	0.32	[104
Methyl cellulose	$Mg(CH_3COO)_2$	2.6×10^{-5}	RT	-	3.47	-	[105]
I-carrageenan	$Mg(ClO_4$	2.18 ×	RT	0.05	-	0.313	[106
Chitosan	$MgCl_2$	$4.6 \times 10^{-}$	-	-	-	-	[107
Pectin	$Mg(NO_3$	$7.7 \times 10^{-}$	RT	-	3.8	0.29	[108
Pectin	$MgCl_2$	1.14 ×	RT	-	2.05	0.301	[109
PEO-PVDF	MgTFSI	$1.2 \times 10^{-}$	25	-	-	-	[111
PEO/PVDF-	$MgBr_2$	$3.9 \times 10^{-}$	RT	0.26	1.86	-	[112
PVA-PAN	$Mg(ClO_4$	2.94 ×	RT	0.21	3.65	0.27	[113
PVDF-HFP+ PVAc	$Mg(ClO_4)_2$	1.60×10^{-5}	30	0.33	3.5	-	[114]
PVP-PVA	$Mg(NO_3$	$3.8 \times 10^{-}$	30	0.475	-	-	[115
PVA-PAN	$MgCl_2$	1.01 ×	RT	0.07	3.66	-	[116
Poly(VdCl-co-AN-co-MMA)	$Mg(NO_3)_2$	1.6×10^{-4}	RT	0.19	3.2	0.36	[117]
PEO/PO	Mg(TFSI	$1.5 \times 10^{-}$	30	-	-	-	[118
PCL-PTMC	Mg(TFSI	2.52 ×	25	-	-	-	[119
PVA-PAN	$Mg(NO_3$	1.71 ×	RT	0.36	3.4	0.30	[120
PVDF-	$Mg(ClO_4$	3.85 ×	30	3.37	3.68	-	[121
CS+MC	$MgCl_2$	2.75 ×	30	-	3.86	-	[122
Corn silk+PVA	$MgCl_2$	1.28 ×	RT	-	2.11	0.32	[123
Methyl cellulose-PVA	$Mg(NO_3)_2$	3.25×10^{-4}	27	-	2.62	-	[124]
PEO-Starch	$MgBr_2$	$7.8 \times 10^{-}$	RT	-	-	-	[125

2.2.2. Polymer electrolytes with plasticizers (Gel-polymer electrolytes)

In general, plasticizers are used to soften a material, to increase its plasticity and to decrease its viscosity. In polymer electrolytes, plasticizers lower T_g (glass-transition temperature) and activate segmental motion of polymer chains, enhancing ionic conductivity. Studies on all-solid-state Mg batteries have been done using GPEs the most.

As Li^+-ion conductive polymer electrolytes, low molecular weight solvents and ionic liquids have been used as a plasticizer (Figure 6). Because plasticizers soften SPEs, optimum amount of plasticizers must be found to balance ionic conductivity and mechanical properties of GPEs. The optimum amount of plasticizers varies significantly by the plasticizers used. In the GPE using $PYR_{14}TFSI$ ionic liquid, the highest ionic conductivity was obtained at 10 wt.% of plasticizer [127]. Contrarily, the plasticizer amount of 200 wt.% was reported in TEGDME system [128]. In such high

Preprints (www.preprints.org) | NOT PEER-REVIEWED | Posted: 10 October 2023 doi:10.20944/preprints202310.0484.v1

plasticizer content, it is questioned whether the ionic conduction is mainly caused by the segmental motion of polymer or dissolved Mg salt in the liquid part.

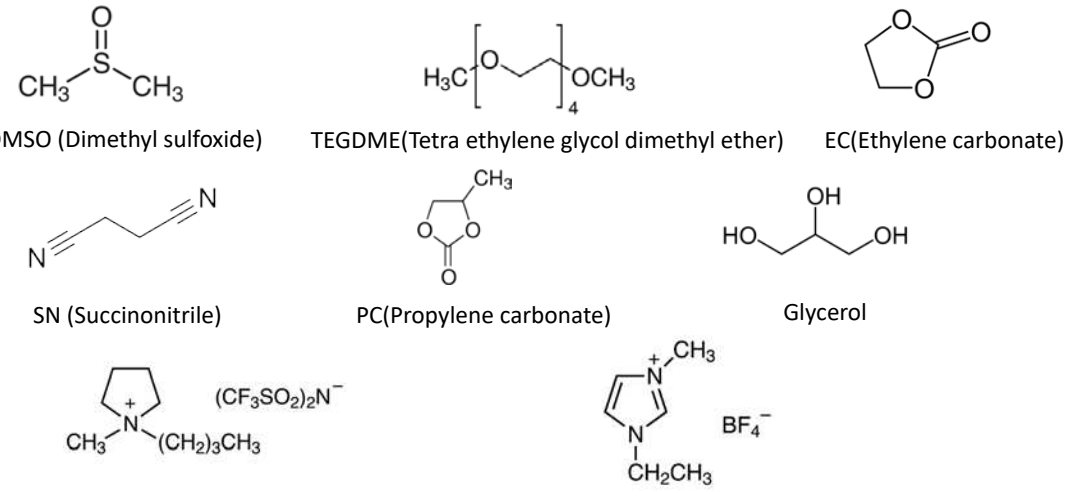

Figure 6. Structures of various plasticizers used in Mg^{2+} ion conductive polymer electrolytes.

In GPEs, synthetic polymers are mostly studied. Their conductivity ranges from 10^{-4} to 10^{-3} S cm^{-1} which can be applied for all-solid-state batteries. Gupta et.al. reported high ionic conductivity of 2 × 10^{-2} S cm^{-1} in [PVdF-HFP(30wt.%)-EMIMBr(70 wt.%)](30 wt.%)-[PC-$Mg(ClO_4)_2$ (0.3 M)] (70 wt.%)system [129]. However, cell data was not reported although the high ionic conductivity is promising. Mixed plasticizers like EC-SN[130] and EC-DEC[131] also have been studied, but they did not improve properties comparing with single plasticizers significantly.

The inorganic magnesium aluminum chloride complex ($MgCl_2$-$AlCl_3$, MACC) has been studied in liquid electrolytes [132]. By the addition of $AlCl_3$, dissociation of $MgCl_2$ is promoted, increasing solubility of $MgCl_2$ and Mg^{2+}-ion concentration. As a result, Mg stripping/plating over potential can be drastically decreased [133]. Wang et. al. applied this concept to GPEs for the first time [134]. The ionic conductivity of their PVDF-HFP-based GPEs containing $MgCl_2$-$AlCl_3$ salt and TEGDME plasticizer was 4.7 × 10^{-4} S cm^{-1}. Although this value was comparable to other GPEs, the reversibility of Mg stripping/plating was drastically improved. In polymer electrolyte research, an effect of Mg salt has not been studied intensively. Their results clearly show the importance of Mg salt on performance of all-solid-state Mg batteries.

As another important study, single-ion conductive polymer electrolyte is reported by Schaefer et. al. [135] In the single-ion conductive polymer electrolyte, anion part of Mg salt is polymerized with host polymers. Thus, mobility of anion is zero, in other words, cation transference number is 1. Therefore, undesired side reactions caused by anions can be avoided completely. The authors prepared P(PEGDMA)-P(TFSI) [poly (ethylenglycol) dimethacrylate- poly styrensulfonyl (trifluoromethylsulfonyl)] network (Figure 7). In this structure, TFSI moiety is involved in the polymer chain, resulting in immobilization of anion. This type of polymer generally shows low ionic conductivity due to low segmental motion of polymer chain. Thus, DMSO plasticizer was added and the Mg^{2+}-ion conductivity was increased to 8.8 × 10^{-4} S cm^{-1}. It is noted that the high conductivity was achieved by only Mg^{2+}-ion transportation. Some other studies reported higher conductivities, however, the comductivities contain anion transportation. Therefore, the high Mg^{2+}-ion conductivity of single-ion conductive polymer is very attractive. Unfortunately, cell data was not reported.

Preprints (www.preprints.org) | NOT PEER-REVIEWED | Posted: 10 October 2023 doi:10.20944/preprints202310.0484.v1

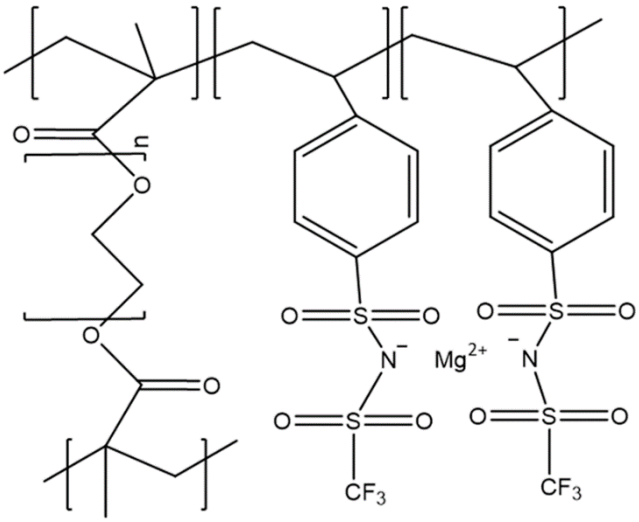

Figure 7. Structures of magnesiated P(PEGDMA)-P(STFSI) network.

In GPEs, mixed salt like MACC and the single-ion conductive polymer are studied. Such studies have been carried out only in GPEs. Their superior properties are promising to apply for all-solid-state Mg batteries. This concept should be investigated intensively and also used in other types of polymer electrolytes such as organic-inorganic composite electrolytes.

Table 6. Properties of GPEs.

Polymer	Mg salt	Plasticizer	σ_{total} (S cm^{-1})	Temp. (°C)	E_a (eV)	Window (V vs. Mg/Mg^{2+})	Transference number	Ref
P(PEGDMA)-P(STFSI)		DMSO	8.8×10^{-4}	30	-	1.5	(1.0)	[135]
PVDF	$Mg(SO_3CF_3)$	TEGDME	4.6×10^{-4}	55	0.62	1.0	0.74	[136]
PEO	$Mg(Tf)_2$	$PYR_{14}TFSI$	3.7×10^{-4}	RT	-	-	0.40	[127]
PEO	$Mg(Tf)_2$	EMIM-BF_4	9.4×10^{-5}	RT	0.26	4.0	0.22	[137]
PVdC-co-AN	$Mg(TFSI)_2$	EC+SN	1.9×10^{-6}	RT	0.04	3.8	0.59	[130]
PVdC-co-AN	$Mg(TFSI)_2$	SN	1.6×10^{-6}	RT	0.09	3.2	-	[138]
PVDF-HFP	$Mg(ClO_4)_2$	EDiMIMB	8.4×10^{-3}	RT	0.33	-	-	[139]
PVDF-HFP	$Mg(ClO_4)_2$	EMIMBr,	2.0×10^{-2}	RT	0.02	-	-	[129]
PEC	$Mg(TFSI)_2$	TEGDME	5.2×10^{-6}	80	-	-	-	[140]
PECH-OH	$MgCl_2$	TEGDME	6.2×10^{-5}	30	0.25	3.2	0.79	[128]
PVDF-HFP	$Mg(Tf)_2$	SN+EMIT	4×10^{-3}	26	0.104	4.1	-	[141]
Poly(VdCl-co-An-co-MMA)	$MgCl_2$	SN	1.4×10^{-3}	RT	0.26	3.3	0.31	[142]
c-PTHF	$Mg(TFSI)_2$	TEGDME	4.5×10^{-5}	30	-	-	-	[143]
CS	$Mg(CH_3COO)_2$	glycerol	1.1×10^{-4}	RT	-	-	-	[144]
k-carrageenan	$Mg(NO_3)_2$	EC	7.3×10^{-3}	30	-	4.59	0.39	[145]
PVDF-	$Mg(ClO_4)_2$	EMITF	9.1×10^{-4}	30	0.28	3.59	-	[146]

Preprints (www.preprints.org) | NOT PEER-REVIEWED | Posted: 10 October 2023 doi:10.20944/preprints202310.0484.v1

Hydroxy	$Mg(TFSI)_2$	TEGDME	$1.73 \times 10^{-}$	25	-	-	-	[147]
PVDF-HFP	$Mg(Tf)_2$	EC-DEC	2.4×10^{-4}	70	-	5.0	0.42	[131]
PVDF	$Mg(ClO_4)_2$	PC	1.5×10^{-3}	RT	-	5.0	0.47	[148]
PVDF-HFP	$Mg(ClO_4)_2$	TEGDME	9.8×10^{-4}	RT	-	4.6	-	[149]
PTHF	MgBOR		2.0×10^{-3}	25	-	2.57	0.3	[150]
PVA	$Mg(Tf)_2$	EMITf	1.2×10^{-3}	RT	-	-	-	[151]
PVDF-HFP	$Mg(ClO_4)_2$	PC	1.6×10^{-3}	RT	-	5.5	-	[152]
PAN	$Mg(ClO_4)_2$	PC	3.3×10^{-3}	30	0.1	4.6	0.6	[153]
PVDF-HFP	$MgCl_2$-	TEGDME	4.7×10^{-4}	25	-	3.1	-	[134]
PEO	$Mg(Tf)_2$	PC-DEC	3.0×10^{-5}	RT	0.14	3.5	0.32	[154]
CS:Dextran	$Mg(CH_3CO$	Glycerol	1.2×10^{-6}	RT	-	1.5	-	[155]

2.2.3. Organic crystal electrolytes

Recently, Moriya's group reported a new type of organic electrolyte, organic crystal electrolytes. They are composed of organic molecules and Mg salts and possess ion conduction paths in the crystal lattice (Figure 8). The paths are precisely controlled by organic molecules and Mg salts. Only two Mg ion conductive organic crystal electrolytes have been reported so far [156,157]. In both cases, room temperature conductivities were higher or comparable to $Mg(BH_4)_2$-based inorganic electrolytes and the cation transference number was higher than that of polymer-based electrolytes. These properties would be improved by adjusting the ion conduction paths. Unfortunately, cell data using the organic crystal electrolytes are not available at the moment. There is still a lot of room to develop organic crystal electrolytes.

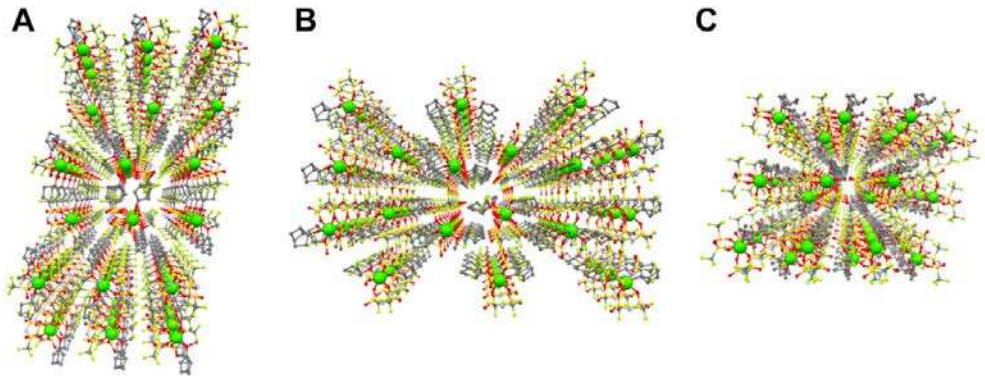

Figure 8. Packing view with ball and stick model of $Mg(TFSA)_2(CPME)_2$. Mg-ions are emphasized as a large sphere. (A) along the a-axis. (B) along the b-axis, and (c) along the c-axis (Mg: green, C: gray, N: pale blue, O: red, F: pale green, S: dark yellow. H atoms are omitted for clarity). Reproduced with permission [156]. Copyright 2021, Frontiers.

Table 6. Properties of organic crystals.

Crystal	σ_{total} (S cm^{-1})	Temp. (°C)	E_a (eV)	Transference number	Ref
$Mg(TFSA)_2(CPME)_2$	2×10^{-7}	30	0.72	0.74	[156]
$[N_{1122}][Mg(\eta^2\text{-}TFSA)_2(\mu_2\text{-}\eta^1\text{-}\eta^1\text{-}TFSA)]$	$2.5 \times 10^{-}$	40	1.21	0.46	[157]

2.3. Organic-inorganic composite electrolytes

Preprints (www.preprints.org) | NOT PEER-REVIEWED | Posted: 10 October 2023 doi:10.20944/preprints202310.0484.v1

2.3.1. Solid polymer electrolytes with fillers

In the Li^+ ion conductive polymer electrolytes, various types of fillers such as organic/inorganic fillers and active/passive (Li^+ ion conductive/non- Li^+ ion conductive) fillers are researched. Contrarily, in the Mg^{2+} ion conductive polymer electrolytes, only inorganic passive fillers, especially metal oxides, are studied. In addition, only nano-particle morphology, not nano-wire, nano-sheet, etc. is employed. Among the studies, the highest conductivity was obtained in filler contents of 3 ~7 wt.% regardless of the fillers. An interesting study was carried out by Jayanthi et. al. in which ferroelectric material, $BaTiO_3$, was added to PVDF-HFP/MgTf polymer electrolyte as a filler [158]. The presence of ferroelectric domains in the polymer electrolyte facilitates salt dissociation and helps amorphization of the polymer, resulting in enhancement of ionic conductivity. Similar study was reported in Na^+ ion conductive polymer electrolyte [159]. In this case, $K_{0.5}Na_{0.5}NbO_3$ (KNN) was used as a ferroelectric filler and it decreased ionic conductivity of polymer electrolyte while stability against Na metal anode was improved. As a result, better performance of all-solid-state Na battery was obtained. This is a good result that the performance of electrolytes is determined by not only conductivity but also interface properties between electrodes and electrolytes. Thus, electrolyte study must include construction and evaluation of all-solid-state battery. Unfortunately, studies on only solid electrolytes have been reported much more than all-solid-state batteries.

Table 7. Properties of SPEs with fillers.

Polymer	Mg salt	Filler	σ_{total} (S cm^{-1})	Temp. (°C)	E_a (eV)	Window (V vs. Mg/Mg^{2+})	Transference number	Ref
PVA/PVP	$MgCl_2$	CuS	4.3 ×	RT	-	-	-	[160]
MC	$MgCl_2$	ZnO	1.2 ×	RT	-	-	-	[161]
PVDF	$Mg(NO_3)_2$	MgO	1.0 ×	RT	0.32	-	-	[162]
PEG	$Mg(CH_3COO)_2$	CeO_2	3.4 ×	RT	-	-	-	[163]
PMMA	$Mg(Tf)_2$	TiO_2	1.8 ×	RT	-	-	-	[164]
CS	$Mg(NO_3)_2$	MnO_2	1.2 ×	30	-	1.7	-	[165]
PVDF-HFP	$Mg(Tf)_2$	$BaTiO_3$	4.1 ×	RT	-	-	-	[158]
PEO	$Mg(Tf)_2$	MgO	1.6 ×	25	0.14	-	-	[166]
PVDF	$Mg(NO_3)_2$	Al_2O_3	9.5 ×	RT	-	-	-	[167]
PVDF	$Mg(NO_3)_2$	ZnO	5.2 ×	RT	0.29	-	-	[168]
PEO	$MgCl_2$	B_2O_3	7.2 ×	25	-	-	-	[169]
PVDF-	$Mg(ClO_4)_2$	$MgTiO_3$	5.8 ×	30	0.25	4.0	0.34	[170]
CS	$MgCl_2$	V_2O_5	1.4 ×	RT	-	1.7	-	[171]
PVDF-HFP	$MgClO_4$	ZrO_2	6.6 ×	30	-	-	-	[172]
PVDF-HFP	$MgCl_2$	ZnO	1.3 ×	RT	-	-	-	[173]

2.3.2. Solid polymer electrolytes including plasticizers and fillers

In this system, polymer electrolytes contain both inorganic fillers and plasticizers. As mentioned, low molecular weight solvents and ionic liquids are employed as a plasticizer. Contrarily, metal oxides are used as a filler. Aziz et. al. used Ni metal nanoparticles as a filler [174]. Metal fillers have not been applied for Mg^{2+}-ion conductive polymer electrolytes except this paper. To clarify effect of metal filler, more research is needed. Sharma et. al. added EC-PC and $MgAl_2O_4$ into PVDF-HFP/$Mg(Tf)_2$ polymer electrolyte [177]. This system revealed high transference number of 0.66 which is one of the highest transference number in Mg^{2+}-ion conductive polymer electrolytes.

Preprints (www.preprints.org) | NOT PEER-REVIEWED | Posted: 10 October 2023 doi:10.20944/preprints202310.0484.v1

The ionic conductivity of filler/plasticizer-containing polymer electrolytes ranges 10^{-5} to 10^{-3} S cm^{-1}. These values are comparable to other types of polymer electrolytes. Thus, benefits of usage of both plasticizers and fillers cannot be emphasized. Currently, individual effect of plasticizers and fillers on properties of polymer electrolytes has yet to be fully understood. Thus, the individual effect of plasticizers and fillers must be clarified at first. Then, more complicated system, i.e. polymer electrolytes containing both plasticizers and fillers, should be developed based on the individual effect.

Table 8. Properties of SPEs with plasticizers and fillers.

Polymer	Mg salt	Plasticizer	Filler	σ_{total} (S	Temp. (°C)	E_a (eV)	Window (V vs. Mg/Mg^2	Transference number	Ref
CS/MC	$Mg(CH_3CO$	Glycerol	Ni	1.0	RT	-	2.48	-	[174]
PEO	$Mg(ClO_4)_2$	EMIMFS	SiO_2	5.4	RT	0.36	4.0	-	[175]
CS	$Mg(CH_3CO$	Glycerol	Ni	1.1	RT	-	2.4	-	[176]
PVDF-	$Mg(Tf)_2$	EC-PC	$MgAl_2$	4.0	RT	-	-	0.66	[177]
PVDF-	$Mg(ClO_4)_2$	$PTR_{14}RF$	TiO_2	1.6	30	0.13	-	0.23	[178]
PVDF-	$Mf(TFSI)_2$	TEGDM	SiO_2	8.3	RT	-	-	-	[179]
PTHF	$Mg(BH_4)_2$-	diglyme	TiO_2	4.2	40	0.00	-	0.5	[180]

3. All-solid-state Mg battery

3.1. Inorganic electrolyte

Research on all-solid-state Mg battery using oxide-based electrolytes is not reported. The Mg^{2+}-ion conductivity of the oxide electrolytes is 10^{-6} ~ 10^{-7} S cm^{-1} at room temperature. This is too low to support ion conduction in all-solid-state batteries operated at room temperature. Thus, improvement of room temperature ionic conductivity to at least 10^{-4} S cm^{-1} level is needed at first. In the case of $MgSc_2Se_4$-related materials, although they possess high Mg^{2+}-ionic conductivity, their electronic conductivities are also high. Thus, these materials are not studied for electrolytes for all-solid-state batteries.

All-solid-state Mg batteries using inorganic electrolytes are reported only in borohydride electrolytes, i.e. $Mg(BH_4)_2$-related materials. While these materials demonstrate good Mg stripping/plating behaviors [62,64,65,67,69], only two papers are reported with respect to full cell configurations. In both cases, TiS_2 is used as a cathode and electrochemical tests were carried out above room temperature to obtain reasonable capacity. The obtained discharge capacity was about 100 mAh/g although the C rate was low. Also, capacity decay occurs rapidly. TiS_2 cathode exhibits large (> 100 mAh/g) and stable (> 100 cycles) capacities at room temperature at reasonable C rate (1 ~ 2 C) in liquid electrolytes [132]. Thus, the low performance of all-solid-state battery would be caused low conductivity of solid electrolyte and high impedance/low stability of cathode/electrolyte interface.

As mentioned, improvement of room temperature ionic conductivity is needed to realize all-solid-state Mg batteries using inorganic electrolytes. Additionally, various cathode materials and properties of electrode/electrolyte interface must be tested and characterized, respectively. In summary, all-solid-state Mg batteries using inorganic electrolytes are still far from realization.

3.2. MOF

Preprints (www.preprints.org) | NOT PEER-REVIEWED | Posted: 10 October 2023 doi:10.20944/preprints202310.0484.v1

In the all-solid-state Mg batteries using MOF-based electrolytes, since MOFs are used to support liquid electrolytes, they can be said "Quasi-solid electrolytes". Although stable Mg stripping/plating is observed, only one paper reported in the full cell configuration. The full cell using PTCDA (Perylenetetracarboxilic dianhydride) cathode demonstrates small discharge capacity of 36 mAh/g. The PTCDA cathode is employed for Na and K batteries [181, 182] and reveals a good performance. However, it has not been applied for Mg batteries even including liquid electrolytes. Therefore, the poor performance of all-solid-state Mg batteries using MOF-based quasi-solid electrolyte is attributed to some factors such as cathode itself, cathode/electrolyte interface, electrolyte itself and so on. Usage of common cathode materials like MoS_6 can reduce the factors, facilitating the evaluation of all-solid-state Mg batteries. Consequently, the common cathode materials should be used for the MOF-based quasi-solid electrolytes at this moment.

Since stable Mg stripping/plating was achieved at room temperature in MOF-based solid electrolytes, they would be promising for all-solid-state Mg battery applications. Therefore, studies on cathode side must be carried out intensively.

3.3. Organic electrolyte

Although studies on SPEs (without fillers and plasticizers) are reported by many groups, SPEs are not applied for all-solid-state Mg batteries. Some groups studied primary Mg batteries using SPEs [90,95,99,106,108,109,113,120,122,124,145]. Since this review article focuses on rechargeable all-solid-state Mg batteries, the studies on primary batteries are not introduced here. The main reason for lack of research on SPEs for rechargeable all-solid-state Mg batteries is their relatively low ionic conductivity. The conductivity of most SPEs ranges 10^{-5} ~ 10^{-7} S cm^{-1} at RT. Improvement of the conductivity to 10^{-3} ~ 10^{-4} S cm^{-1} at least is needed to achieve reasonable performance of all-solid-state Mg batteries. Potato starch [94] and Gellun gum [97]-based SPEs exhibit extremely high ionic conductivity of ~10^{-2} S cm^{-1}. These are 2 orders of magnitude higher than other SPEs. Close investigation for these SPEs, such as reproducibility and characterization procedures, should be performed since such very high conductivity of these SPEs cannot be accepted easily.

3.3.1. Gel polymer electrolyte

Gel polymer electrolytes (GPEs) composed of post polymers, Mg salts and plasticizers possess higher conductivity, 10^{-3} ~ 10^{-4} S cm^{-1}, than SPEs. Additionally, their high flexibility makes battery construction easy. Thus, all-solid-state Mg batteries using GPEs are reported the most. The all-solid-state Mg batteries using GPEs can be operated at room temperature [128, 134, 141, 150]. However, in all cases, initial and steady-state capacities are low. Because stable Mg stripping/plating is observed in GPEs, cathode itself and cathode/electrolyte interface would be the reason for the low performance. Detail characterization and post-mortem analysis of the interface and cathode should be carried out.

Ge et. al. fabricates pouch cell-type all-solid-state Mg batteries for the first time [128]. Only this study reports the performance of pouch cell-type all-solid-state Mg battery with GPE. The pouch cell can reduce a weight of battery cases, resulting in high energy density. Additionally, the authors performed safety tests, such as cutting the pouch cell and flammability tests of GPE and pouch cell. The study is meaningful in verifying the possible application of pouch cell configuration for all-solid-state Mg batteries, although improvement of performance of the pouch cells is needed.

Sheha et. al. studies dual polymer/liquid electrolyte (Figure 9) [136]. The electrolyte is composed of two layers, liquid electrolyte and GPE. Both electrolytes are separated by a glass fiber membrane. The liquid electrolyte (APC, all phenyl complex) and GPE are faced on cathode and anode (Mg metal) sides, respectively. In the all-solid-state battery, a poor contact between porous electrode and solid electrolyte increases impedance of the battery and causes low performance. At the moment, effective solution of the contact issue has yet to be found. Their concept would be helpful in solving the contact issue. Therefore, the dual electrolyte configuration is likely to be applied for first generation all-solid-state Mg batteries. The authors report high initial capacity using $BaTiO_3$ cathode, but the capacity is rapidly decayed within 15 cycles. The reason for low cyclability is unclear since cyclability of $BaTiO_3$ cathode has not been tested in liquid electrolytes. The dual electrolytes should be studied using

Preprints (www.preprints.org) | NOT PEER-REVIEWED | Posted: 10 October 2023 doi:10.20944/preprints202310.0484.v1

common cathode materials at first. For safety, usage of the flammable liquid electrolytes must be minimized. Influence of the liquid electrolyte on safety of the batteries, formation of CEI (cathode-electrolyte interphase) and properties of new interface, i.e. GPE/liquid electrolyte should be studied for successful application of the dual electrolyte system (In fact, the battery is not pure all-solid-state Mg batteries since the batteries contain a small amount of liquid electrolyte).

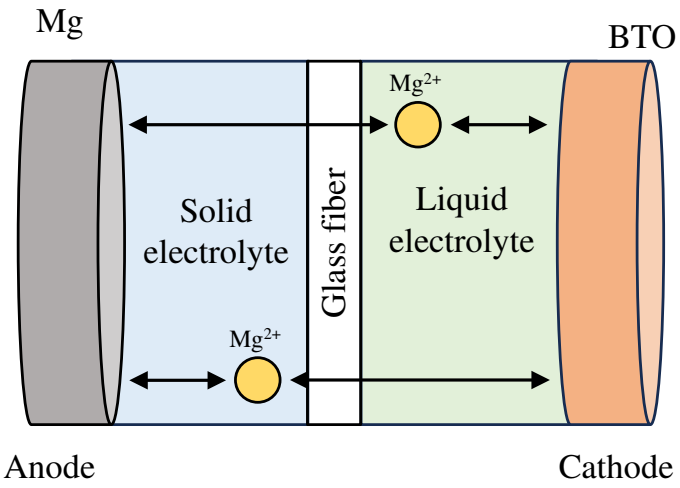

Figure 9. Configuration of Mg battery using the dual GPE/liquid electrolyte (Mg/GPE/APC/$BaTiO_3$ cathode). Reproduced with permission [136]. Copyright 2020, American Chemical Society.

In the GPE research, Mo_6S_8 which is the most commonly used cathode material, is applied for the all-solid-state battery [128, 150]. This facilitates evaluation of the all-solid-state batteries since performance of cathode is studied in liquid electrolytes for long time. Mo_6S_8 cathode provides high capacity (130 mAh g^{-1} at 0.1 C and 98 mAh g^{-1} at 0.5 C) in liquid electrolytes [183, 184]. Contrarily, the all-solid-state batteries using GPEs demonstrate about 70 mAh g^{-1} (68 mAh g^{-1} at 0.1 C [150] and 73 mAh g^{-1} at 0.3 C [128]) even though same cathode materials are used. Because ionic conductivity of electrolytes would not largely influence battery performance at such low C rate, high impedance at cathode-electrolyte interface could be a reason for the low performance. Common electrode materials should be used for all-solid-state batteries more intensively. It is interesting to note that better battery performance was obtained in the PECH-OH-based GPE comparing to the PTHF-based GPE. As shown in Table 6, the PTHF-based GPE revealed about 2 order of magnitude higher Mg^{2+}-ion conductivity than the PECH-OH-based GPE. This is a good example that battery performance is determined by not only properties of electrolytes. GPE is the most promising for all-solid-state Mg batteries at this moment. The ionic conductivity of GPEs is comparable to Li^+-ion conductive polymer electrolytes. Thus, compatibility with electrodes and properties of electrode/electrolyte interface would determine the performance of all-solid-state Mg batteries. Many studies on GPEs are reported, while their application to all-solid-state Mg batteries is seldom researched. Such study is strongly required, not only simply study on properties of GPEs, to realize all-solid-state Mg batteries.

3.4. Organic-inorganic composite electrolytes

Only 3 papers have been reported in terms of all-solid-state Mg batteries using the organic-inorganic composite electrolytes recently [170,179,180]. Comparing with GPEs, all-solid-state Mg batteries with the composite electrolytes demonstrate better initial performance and cyclability. Particularly, when SPEs contain both fillers and plasticizers, very stable cyclability was achieved although only 2 papers were reported. The compatibility of polymer electrolytes with electrodes, especially cathodes, is likely to be improved by adding fillers. Wang et al. successfully prepared the pouch cell-type all-solid-state Mg batteries [180]. The cell demonstrated excellent performance. However, the solid electrolyte contains two salts, $Mg(BH_4)_2$ and $LiBH_4$. The ratio of Mg/Li is 0.1/1.5. Thus, it is unclear influence of Li intercalation on observed capacity.

Preprints (www.preprints.org) | NOT PEER-REVIEWED | Posted: 10 October 2023 doi:10.20944/preprints202310.0484.v1

Despite fewer examples, fillers would improve the stability of all-solid-state Mg batteries. Application of the organic-inorganic composite electrolytes for all-solid-state Mg batteries must be studied more intensively. Although pouch cell-type all-solid-state battery was reported, common coin cell configuration and cathode materials should be adopted at this moment because the application of organic-inorganic composite electrolytes for all-solid-state Mg battery is still infant stage.

Table 9. Properties of all-solid-state Mg batteries.

Electrolyte	Cathode	Initial capacity	Capacity retention	Temp.	Note	Ref
Borohydrides						
$Mg(BH_4)(NH_2)$	Pt	-	-	-	Mg plating on Pt	[62]
$Mg(BH_4)(NH_3BH_3)_2$	Mo	-	-	-	Mg plating on Mo	[65]
$0.4Mg(BH_4)2•NH_3$-$0.6Mg(BH_4)_2•2NH_3$@	Mg	-	-	60	Stable Mg stripping/plating more than 100 cycles at 0.25 mA cm^{-2}	[69]
$Mg(en)_1(BH_4)_2$	Pt	-	-	60	Stable Mg stripping/plating in	[64]
$Mg(BH_4)_2$ 1.5NH_3-	Mg	-	-	60	Stable Mg stripping/plating in	[67]
$Mg(BH_4)•2NH_3$	TiS_2	141 mAh/g at 0.05C	31 % at 25th cycle	75	111 mAh/g at 0.2C, 72 mAh/g at 0.5C	[73]
$Mg(BH_4)_2$•1.5THF-MgO	TiS_2	94 mAh/g at C/50	32 % at 5th cycle	55	SS current collector was oxidized	[70]
MOF						
$Mg(TFSI)_2/MgCl_2$/DME in MOF-74	Mg	-	-	RT	Stable Mg stripping/plating in 100 cycles at 0.05	[79]
Mgbp3dc in α-$Mg_3(HCOO)_6$/DMF	Mg	-	-	RT	Stable Mg stripping/plating in	[76]
$Mg(TFSI)_2$/[EMIM][TFSI] in UiO-66	PTCDA	36 mAh/g at 1	61 % at 3rd cycle	60	Stable Mg stripping/plating more than 200 cycles	[77]
GPE						
PVDF-TEGDME-$Mg(Tf)_2$	$BaTiO_3$	557 mAh/g at 20 mA/g	12 % at 15th cycle	55	●Full cell configuration: Mg/SE/APC/Cathode ●Stable Mg	[136]
PECH-OH-$MgCl_2$-TEGDME	Mo_6S_8	73 mAh/g at 0.3 C	84 % at 100th cycle	30	Pouch cell data	[128]
PVDF-HFP-$Mg(Tf)_2$-SN+EMITf	MnO_2	40 mAh/g at 38 μA	12.5 % at 8th cycle	RT		[141]
PTHF-MgBOR	Mo_6S_8	68 mAh/g at 0.1 C	74 % at 100th cycle	25	Stable Mg stripping/plating more than 1000 cycles at 0.1 mA cm^{-2}	[150]
PVDF/HFP-$MgCl_2/AlCl_3$-TEGDME	MoS_2	121 mAh/g at 40 mA/g	58 % at 1700th cycle	25	Stable Mg stripping/plating more than 400 cycles at 1.0 mA cm^{-2}	[134]
Filler						
PVDF-HFP/PVAc-$Mg(ClO_4)_2$-$MgTiO_3$	Mo_6S_8	120 mAh/g at 0.5 C	87 % at 30th cycle	RT		[170]
SPE+filler+plasticizer						

 doi:10.20944/preprints202310.0484.v1

PVDF-HFP-$Mg(TFSI)_2$-SiO_2	TiO_2	129 mAh/g at 50	99 % at 100th cycle	RT	Stable Mg stripping/plating more than 100 cycles	[179]
PTHF-$Mg(BH_4)_2$/$LiBH_4$-Diglyme-	TiS_2	225 mAh/g at 0.5 C	98 % at 70th cycle	22	Stable Mg stripping/plating more than 100 cycles	[180]

4. Challenges

The all-solid-state Mg battery is a good option to replace LIBs due to high safety, energy density and resource abundance. Thanks to many efforts of researchers, technologies for the all-solid-state Mg battery have progressed significantly. Despite the significant progress, further research is still required to realize the all-solid-state Mg battery. Herein, challenges are summarized.

(1) Inorganic electrolytes

The Mg^{2+}-ion conductivity of current inorganic electrolytes are 10^{-6} ~ 10^{-7} S cm^{-1} at room temperature in ceramic electrolytes (except weird results [33, 35, 59]). Even hydride-based inorganic electrolytes, the conductivity is ~10^{-5} S cm^{-1}. For all-solid-state Mg batteries, required conductivity is > ~10^{-4} S cm^{-1} at room temperature to ensure room temperature operation. Thus, improvement of ionic conductivity must be investigated in inorganic electrolytes. Some groups have studied Mg^{2+}-ion conductivity of ceramic electrolytes intensively, however, effective solution to enhance the conductivity is yet to be found at this moment. Thus, thin film ceramic electrolytes would be effective to compensate the low conductivity. Currently, only one paper is reported with respect to thin film ceramic electrolytes [58]. The thin film ceramic electrolytes should be studied more intensively. In the hydride-based electrolytes, addition of inorganic fillers is likely to improve the ionic conductivity effectively [67,68]. The effect of fillers should be researched.

(2) Study on Mg salts

Comparing to the inorganic electrolytes, organic polymer electrolytes are more promising in application of all-solid-state Mg battery at this moment. Various polymer hosts have been studied. On the other hand, systematic study on Mg salts is not carried out. Fichtner et. al. reported corrosion of battery case and current collectors by Cl-contained salt [150]. Although various types of Mg salts such as $MgSO_4$, $MgCl_2$, $Mg(ClO_4)_2$, $Mg(TFSI)_2$, $Mg(NO_3)_2$, $Mg(Tf)_2$, have been employed so far, suitable Mg salt for the all-solid-state Mg battery is still under investigation. Therefore, effect of Mg salts on properties of SPEs (and GPEs) and performance of all-solid-state Mg batteries should be studies systematically.

(3) Mechanical properties of solid electrolytes

High flexibility is one of the benefits of SPEs and GPEs which facilitates construction of the all-solid-state Mg battery. However, quantitative evaluation of the flexibility, i.e. mechanical properties has not been carried out yet. The mechanical properties of solid electrolytes influence cell pressure, contact with electrodes, suppression of Mg dendrite formation, etc. significantly. Consequently, both electrochemical and mechanical properties of SPEs and GPEs must be characterized precisely.

(4) Construction of all-solid-state Mg battery

As mentioned in previous section, most research focus on solid electrolyte and only some papers try to fabricate all-solid-state Mg batteries. Compatibility of solid electrolytes with all-solid-state Mg battery cannot be evaluated by not only ionic conductivity, electrochemical window, transference number, etc. Therefore, solid electrolytes must be evaluated in all-solid-state batteries in addition to the above mentioned properties. Particularly, properties of electrode/solid electrolyte interface which largely affect performance of all-solid-state Mg batteries can be characterized only in the all-solid-state battery configuration.

(5) Cathode materials

Some groups employ novel cathode materials for the all-solid-state Mg batteries. In this case, performance of the cathode material is unknown. Thus, it is impossible to clarify the reason for poor performance of the all-solid-state Mg battery, i.e. cathode itself or other components. Common cathode materials such as Mo_6S_8 and TiS_2 which are well characterized in liquid electrolytes should

 doi:10.20944/preprints202310.0484.v1

be used to characterize and evaluate the all-solid-state Mg batteries. After that, development of cathode materials for all-solid-state batteries would be carried out.

All-solid-state Mg battery would replace current LIBs owing to high safety, energy density and resource abundance although the research is still infant stage. To realize the all-solid-state Mg battery, above mentioned studies must be carried out intensively. Additionally, research on Mg battery using liquid electrolytes should be referred especially for the cathode selection.

Author Contributions: J.P. and G.J.; analysis, writing—original draft preparation, K.Z. and M.K.; writing—review and editing, M.K.; supervision. All authors have read and agreed to the published version of the manuscript.

Funding: This research received no external funding.

Conflicts of Interest: The authors declare no conflict of interest.

References

1. Winter, M.; Barnett, N.; Xu, K. Before Li ion batteries. *Chem. Rev.* **2018**, *118*, 11433-11456.
2. Li, M.; Lu, J.; Chen, Z.W.; Amine, K. 30 years of lithium-ion batteries. *Adv. Mater.* **2018**, *30*, 1800561.
3. Li, Q.; Chen, D.; Tan, H.; Zhang, X.; Rui, X.; Yu, Y. 3D porous V_2O_5 architectures for high-rate lithium storage. *J. Energy Chem.* **2020**, *40*, 15-21.
4. Zeng, J.; Peng, C.; Wang, R.; Cao, C.; Wang, X.; Liu, J. Micro-sized FeS_2@$FeSO_4$ core-shell composite for advanced lithium storage. *J. Alloy Compd.* **2020**, *814*, 151922.
5. Armand, M.; Tarascon, J.M.; Building better batteries. *Nature* **2008**, *451*, 652-657.
6. Whittingham, M.S. Ultimate limits to intercalation reactions for lithium batteries. *Chem. Rev.* **2014**, *114*, 11414-11443.
7. Xu, W.; Wnag, J.L.; Ding, F.; Chen, X.L.; Nasybutin, E.; Zhang, Y,H.; Zhang, J.G. Lithium metal anodes for rechargeable batteries. *Energy Environ. Sci.* **2014**, *7*, 513-537.
8. Wang, Y.; Liang, J.; Song, X.; Jin, Z. Recent progress in constructing halogenated interfaces for highly stable lithium metal anodes. *Energy Storage Mater.* **2023**, *54*, 732-775.
9. Sarkar, S.; Thangadurai, V. Critical current densities for high-performance all-solid-state Li-metal batteries: fundamentals mechanisms, interfaces materials and applications. *ACS Energy Lett.* **2022**, *7*, 1492-1527.
10. Feng, Z.; Kotobuki, M.; Song, S.; Lai, M.O.; Lu, L. Review on solid electrolytes for all-solid-state lithium-ion batteries. *J. Power Sources* **2018**, *389*, 198-213.
11. Hebie, S.; Mgo, H.P.K.; Lepretre, J.-C.; Iojoiu, C.; Cointeaux, L.; Berthelot, R.; Alloin, F. Electrolyte based on easily synthesized, low cost triphenolate-borohydride salt for high performance Mg(TFSI)2-glyme rechargeable magnesium batteries. *ACS Appl. Mater.&Interfaces* **2017**, *9*, 28377-28385.
12. Wei, C.; Tan, L.; Zhang, Y.; Xi, B.; Xiong, S.; Feng, J.; Qian, Y.; Highly reversible Mg metal anodes enabled by interfacial liquid metal engineering for high-energy Mg-S batteries. *Energy Storage Mater.* **2022**, *48*, 447-457.
13. Jackle, M.; Helmbrecht, K.; Smits, M.; Stottmeister, D.; Gross, A. Self-diffusion barriers: possible descriptors for dendrite growth in batteries. *Energy Environ. Sci.* **2018**, *11*, 3400-3407.
14. Kotobuki, M. Recent progress of ceramic electrolytes for post Li and Na batteries. *Funct. Mater. Lett.* **2021**, *14(03)*, 2130003.
15. Shuai, H.; Xu, J.; Huang, K. Progress in retrospect of electrolytes for secondary magnesium batteries. *Coordination Chem. Rev.* **2020**, *422*, 213478.
16. Chen, C.; Wang, K.; He, H.; Hanc, E.; Kotobuki, M.; Lu, L. Processing and properties of garnet-type $Li_7La_3Zr_2O_{12}$ ceramic electrolytes. *Small* **2022**, 2205550.
17. Wang, C.; Fu, K.; Kammampata, S.P.; McOwen, D.W.; Samson, A.J.; Zhang, L.; Hits, G.T.; Nolan, A.M.; Wachman, E.D.; Mo, Y.; Thangadurai, V.; Hu, L. Garnet-type solid-state electrolytes: materials, interfaces and batteries. *Chem. Rev.* **2020**, *120*, 4257-4300.
18. Miao, G.; CHongyang, Y.; Tengfei, Z.; Xuebin, Y. Solid state electrolytes for rechargeable magnesium-ion batteries: From structure to mechanism. *Small* **2022**, *18(43)*, 2106981.
19. Stefania, F.; Marisa, F.; Belen, B.G.A.; Matteo, B.; Segio, B.; Michele, P.; Claudio, G. Solid-state post Li metal ion batteries: A sustainable forthcoming reality? *Adv. Energy Mater.* **2021**, *11(43)*, 2100785.
20. Yan, B.; Wang, Z.; Ren, H.; Lu, X.; Qu, Y.; Liu, W.; Jiang, K.; Kotobuki, M. Interfacial modification of $Na_3Zr_2Si_2PO_{12}$ solid electrolyte by femtosecond laser etching. *Ionics* **2023**, *29*, 865-870.
21. Wang, Y.; Wang, Z.; Zheng, F.; Sun, J.; Oh, J.A.S.; Wu, T.; Chen, G.; Huang, Q.; Kotobuki, M.; Zeng, K.; Lu, L. Ferroelectric engineered electrode-composite polymer electrolyte interfaces for all-solid-state sodium metal battery. *Adv. Sci.* **2022**, 2105849.

22. Nakayama, M.; Nakano, K.; Harada, M.; Tanibata, N.; Takeda, H.; Noda, Y.; Kobatashi, R.; Karasuyama, M.; Takeuchi, I.; Kotobuki, M. Na superionic conductor-type $LiZr_2(PO_4)_3$ as a promising solid electrolyte for use in all-solid-state Li metal batteries. *Chem. Comm.* **2022**, *58*, 9328.
23. Kotobuki, M.; Yanagiya, S. Li-ion conductivity of NASICON-type $Li_{1+2x}Zr_{2-x}Ca_x(PO_4)_3$ solid electrolyte prepared by spark plasma sintering. *J. Alloy Compd.* **2021**, *862*, 158641.
24. Kotobuki, M.; Koishi, M. Preparation of $Li_{1.3}Al_{0.3}Ti_{1.7}(PO_4)_3$ solid electrolyte via a sol-gel method using various Ti Sources. *J. Asian Ceram. Soc.* **2020**, *8*, 891-897.
25. Kotobuki, M.; Koishi, M. Preparation of $Li_{1.5}Al_{0.5}Ti_{1.5}(PO_4)_3$ solid electrolyte via a sol-gel route using various Al sources. *Ceram. Int.* **2013**, *39*, 4645-4649.
26. Hayamizu, K.; Haishi, T. Ceramic-glass pellet thickness and Li diffusion in NASICON-type LAGP ($Li_{1.5}Al_{0.5}Ge_{1.5}(PO_4)_3$) studied by pulsed field gradient NMR spectroscopy. *Solid State Ionics* **2022**, *380*, 115924.
27. Yan, B.; QU, Y.; Ren, H.; Lu, X.; Wang, Z.; Liu, W.; Wang, Y.; Kotobuki, M.; Jiang, K. A solid-liquid composite electrolyte with a vertical microporous $Li_{1.5}Al_{0.5}Ge_{1.5}(PO_4)_3$ skeleton that prepared by femtosecond laser structuring and filled with ionic liquid. *Mater. Chem. Phys.* **2022**, *287*, 126265.
28. Lee, W.; Tamura, S.; Imanaka, N. Synthesis and characterization of divalent ion conductors with NASICON-type structures. *J. Asian Ceram. Soc.* **2019**, *7*, 221-227.
29. Shao, Y.J.; Zhong, G.M.; Lu, Y.X.; Liu, L.L.; Zhao, C.L.; Zhang, Q.Q. A novel NASICON-based glass-ceramic composite electrolyte with enhanced Na-ion conductivity. *Energy Storage Mater.* **2019**, *23*, 514-521.
30. Ikeda, S.; Takahashi, M.; Ishikawa, J.; Ito, K. Solid electrolytes with multivalent cation conduction. 1. Conducting species in $MgZrPO_4$ system. *Solid State Ionics* **1987**, *23*, 125-129.
31. Nakano, K.; Noda, Y.; Tanibata, N.; Nakayama, M.; Kajihara, K.; Kanamura, K. Computational investigation of the Mg-ion conductivity and phase stability of $MgZr_4(PO_4)_6$. *RSC Adv.* **2019**, *9*, 12590-12595.
32. Kawamura, J.; Morota, K.; Kuwata, N.; Nakamura, Y.; Maekawa, H.; Hattori, T.; Imanaka, N.; Okazaki, Y.; Adachi, G.-Y. High temperature ^{31}P NMR study on Mg^{2+} ion conductors. *Solid State Comm.* **2001**, *120*, 295-298.
33. Anuar, N.K.; Adnan, S.B.R.S.; Jaafar, M.H.; Mohamed, N.S. Studies on structural and electrical properties of $Mg_{0.5+y}(Zr_{2-y}Fe_y)_2(PO_4)_3$ ceramic electrolytes. *Ionics* **2016**, *22*, 1125-1133.
34. Tamura, S.; Yamane, M.; Hoshino, Y.; Imanaka, N. Highly conducting divalent Mg^{2+} cation solid electrolytes with well-ordered three-dimensional network structure. *J. Solid State Chem.* **2016**, *235*, 7-11.
35. Anuar, N.K.; Mohamed, N.S. Structural and electrical properties of novel $Mg_{0.9+0.5y}Zn_{0.4}Al_yZr_{1.6-y}(PO_4)_3$ ceramic electrolytes synthesized via nitrate sol-gel method. *J. Sol-Gel Sci. Tech.* **2016**, *80*, 249-258.
36. Halim, Z.A.; Adnan, S.B.R.S.; Mohamed, N.S. Effect of sintering temperature on the structural, electrical and electrochemical properties of novel $Mg_{0.5}Si_2(PO_4)_3$ ceramic electrolytes. *Ceram. Int.* **2016**, *42*, 4452-4461.
37. Su, J.; Tsuruoka, T.; Tsujita, T.; Nishitani, Y.; Nakura, K.; Terabe, K. Aromic layer deposition of a magnesium phosphate solid electrolyte. *Chem. Mater.* **2019**, *31*, 5566-5575.
38. Takeda, H.; Nakano, K.; Tanibata, N.; Nakayama, M. Novel Mg-ion conductive oxide of μ-cordierite $Mg_{0.6}Al_{1.2}Si_{1.8}O_6$. *Sci. Tech. Adv. Mater.* **2020**, *21*, 131-138.
39. Omote, A.; Yotsuhashi, S.; Zenitani, Y.; Yamada, Y. High ion conductivity in $MgHf(WO_4)_3$ solids with ordered structure: 1-D alignments of Mg^{2+} and Hf^{4+} ions. *J. Am. Ceram. Soc.* **2011**, *94(8)*, 2285-2288.
40. Fujii, Y.; Kobayashi, M.; Miura, A.; Rosero-Navarro, N.C.; Li, M.; Sun, J.; Kotobuki, M.; Tadanaga, K. Fe-P-S electrodes for all-solid-state lithium secondary batteries using sulfide-based solid electrolytes. *J. Power Sources* **2020**, *449*, 227576.
41. Yamanaka, T.; Hayashi, A.; Yamauchi, A.; Tatsumisago, M. Preparation of magnesium ion conducting MgS-P_2S_5-MgI_2 glasses by a mechanochemical technique. *Solid State Ionics* **2014**, *262*, 601-603.
42. Canepa, P.; Bo, S.-H. Gautam, G.S.; Key, B.; Richards, W.D.; Shi, T.; Tian, Y.; Wang, Y.; Li, J.; Ceder, G. High magnesium mobility in ternary spinel chalcogenides. *Nat. Comm.* **2017**, *8*, 1759.
43. Koishi, M.; Kotobuki, M. Preparation of Y-doped $Li_7La_3Zr_2O_{12}$ by co-precipitation method. *Ionics* **2022**, *28*, 2065-2072.
44. Wang, L.-P.; Zhao-Karger, Z.; Klein, F.; Chable, J.; Braun, T.; Schuer, A.R.; Wang, C.-R.; Guo, Y.-G.; Fichtner, M. $MgSc_2Se_4$-magnesium solid ionic conductor for all-solid-state Mg batteries? *ChemSusChem* **2019**, *12(10)*, 2286-2293.
45. Kundu, S.; Solomatin, N.; Kauffmann, Y.; Kraytsberg, A.; Ein-Eli, Y. Revealing and excluding the root cause of the electronic conductivity in Mg-ion $MgSc_2Se_4$ solid electrolyte. *Appl. Mater. Today* **2021**, *23*, 100998.
46. Kundu, S.; Solomatin, N.; Kraytsberg, A.; Ein-Eli, Y. $MgSc_2Se_4$ solid electrolyte for rechargeable Mg batteries: An electric field-assisted all-solid-state synthesis. *Energy Tech.* **2022**, *10*, 2200896.
47. Clemenceau, T.; Andriamady, N.; Kumar, M.K.; Bardran, A.; Avila, V.; Dhal, K.; Hopkins, M.; Vendrell, X.; Marshall, D.; Raj, R. Flash sintering of Li-ion conducting ceramic in a few seconds at 850 ^oC. *Scripta Materialia* **2019**, *172*, 1-5.
48. Yan, B.; Kang, L.; Kotobuki, M.; He , L.; Liu, B.; Jiang, K. Boron group element doping of Li1.5Al0.5Ge1.5(PO4)3 based on microwave sintering. *J. Solid State Electrochem.* **2021**, *25*, 527-534.

49. Wang, C.; Ping, W.; Bai, Q.; Cui, H.; Hensleigh, R.; Wang, R.; Brozena, A.H.; Xu, Z.; Dai, J.; Pei, Y.; Zheng, C.; Pastel, G.; Gao, J.; Wang, X.; Wang, H.; Zhao, J.-C.; Yang, B.; Zheng, X.; Luo, J.; Mo, Y.; Dunn, B.; Hu, L. A general method to synthesize and sinter bulk ceramics in seconds. *Science* **2020**, *368*, 521-526.
50. Anuar, N.K.; Adnan, S.B.R.S.; Mohamed, N.S. Characterization of $Mg_{0.5}Zr_2(PO_4)_3$ for potential use as electrolyte in solid state magnesium batteries. *Ceram. Int.* **2014**, *40*, 13719-13727.
51. Mohammed, A.; Kale, G.M. Novel sol-gel synthesis of $MgZr_4P_6O_{24}$ composite solid electrolyte and newer insight into the Mg^{2+}-ion conducting properties using impedance spectroscopy. *J. Phys. Chem. C* **2016**, *120*, 17909-17915.
52. Imanaka, N.; Okazaki, Y.; Adachi, G.-Y. Divalent magnesium ion conducting characteristics in phosphate based solid electrolyte composites. *J. Mater. Chem. C* **2000**, *10*, 1431-1435.
53. Imanaka, N.; Okazaki, Y.; Adachi, G. Optimization of divalent magnesium ion conduction in phosphate based polycrystalline solid electrolytes. *Ionics* **2001**, *7*, 440-446.
54. Liang, B.; Kreshishian, V.; Liu, S.; Yi, E.; Jia, D.; Zhou, Y.; Kieffer, J.; Ye, B.; Kaine, R.M. Processing liquid-feed flame spray pyrolysis synthesized $Mg_{0.5}Ce_{0.2}Zr_{1.8}(PO_4)_3$ nanopowders to free standing thin films and pellets as potential electrolytes in all-solid-state Mg batteries. *Electrochim. Acta* **2018**, *272*, 144-153.
55. Kajihara, K.; Nagano H.; Tsujita, T.; Munakata, H.; Kanamura, K. High-temperature conductivity measurements of magnesium-ion-conducting solid oxide $Mg_{0.5-x}(Zr_{1-x}Nb_x)_2(PO_4)_3$ (x = 0.15) using Mg metal electrodes. *J. Electrochem. Soc.* **2017**, *164(9)*, A2183-A2185.
56. Mustafa, M.; Rani, M.S.A.; Adnan, S.B.R.S.; Salleh, F.M.; Mohamed, N.S. Characteristics of new $Mg_{0.5}(Zr_{1-x}Sn_x)_2(PO_4)_3$ NASICON structured compound as solid electrolytes. *Ceram. Int.* **2020**, *46*, 28145-28155.
57. Imanaka, N.; Okazaki, Y.; Adachi, G. Divalent magnesium ionic conduction in $Mg_{1-2x}(Zr_{1-x}Nb_x)_4P_6O_{24}$ (x = 0-0.4) solid solutions. *Electrochem. Solid State Lett.* **2000**, *3(7)*, 327-329.
58. Liu, S.; Zhou, C.; Wang, Y.; Yi, E.; Wang, W.; Kieffer, J.; Laine, R.M. Processing combustion synthesized $Mg_{0.5}Zr_2(PO_4)_3$ nanopowders to thin films as potential solid electrolytes. *Electrochem. Comm.* **2020**, *116*, 106753.
59. Halim, Z.A.; Adnan, S.B.R.S.; Salleh, F.M.; Mohamed, N.S. Effects of Mg^{2+} interstitial ion on the properties of $Mg_{0.5+x/2}Si_{2-x}Al_x(PO_4)_3$ ceramic electrolytes. *J. Magnesium Alloy* **2017**, *5*, 439-447.
60. Sulaiman, M.; Su, N.C.; Mohamed, N.S. Sol-gel synthesis and characterization of β-$MgSO_4$: $Mg(NO_3)_2$-MgO composite solid electrolyte. *Ionics* **2017**, *23*, 443-452.
61. Matsuo, M.; Oguchi, H.; Sato, T.; Takamura, H.; Tsuchida, E.; Ikeshoji, T.; Orimo, S.-I. Sodium and magnesium ionic conduction in complex hydrides. *J. Alloy Compd.* **2013**, *580*, S98-S101.
62. Higashi, S.; Miwa, K.; Aoki, M.; Takechi, K. A novel inorganic solid state ion conductor for rechargeable Mg batteries. *Chem. Comm.* **2014**, *50*, 1320.
63. Ruyet, R.L.; Berthelot, R.; Salager, E.; Florian, P.; Fleutot, B.; Janot, R. Investigation of $Mg(BH_4)(NH_2)$-based composite materials with enhanced Mg^{2+} ionic conductivity. *J. Phys. Chem. C* **2019**, *123*, 10756-10763.
64. Roedern, E.; Kuhnel, R.-S.; Remhof, A.; Battaglia, C.; Magnesium ethylenediamine borohydride as solid-state electrolyte for magnesium batteries. *Sci. Rep.* **2017**, *7*, 46189.
65. Kisu, K.; Kim, S.; Inukai, M.; Oguchi, H.; Takagi, S.; Orimo, S.-I. Magnesium borohydride ammonia borane as a magnesium ionic conductor. *ACS Appl. Energy Mater.* **2020**, *3*, 3174-3179.
66. Luo, X.; Rawal, A.; Cazorla, C.; Aguey-Zinsou, K.F. Facile self-forming superionic conductors based on complex borohydride surface oxidation. *Adv. Sus. Syst.* **2020**, 1900113.
67. Wang, Q.; Li, H.; Zhang, R.; Liu, Z.; Deng, H.; Cen, W.; Yan, Y.; Chen, Y. Oxygen vacancies boosted fast Mg^{2+} migration in solids at room temperature. *Energy Storage Mater.* **2022**, *51*, 630-637.
68. Yan, Y.; Grinderslev, J.B.; Burankova, T.; Wei, S.; Embs, J.P.; Skibsted J.; Jensen, T.R. Fast room-temperature Mg^{2+} conductivity in $Mg(BH_4)_2$•$1.6NH_3$-Al_2O_3 nanocomposites. *J. Phys. Chem. Lett.* **2022**, *13*, 2211-2216.
69. Yan, Y.; Grinderslev, J.B.; Jorgensen, M.; Skov, L.N.; Skibsted J.; Jensen, T.R. Ammine magnesium borohydride nanocomposites for all-solid-state magnesium batteries. *ACS Appl. Energy Mater.* **2020**, *3*, 9264-9270.
70. Skov, L.N.; Grinderslev, J.B.; Rosenkranz, A.; Lee, Y.-S.; Jensen, T.R. Towards solid-state magnesium batteries: Ligand-assisted superionic conductivity. *Batteries&Supercaps* **2022**, *5*, e202200163.
71. Ruyet, R.L.; Berthelot, R.; Salager, E.; Florian, P.; Fleutot, B.; Janot, R. Investigation of $Mg(BH_4)(NH_2)$-based composite materials with enhanced Mg^{2+} ionic conductivity. *J. Phys. Chem. C* **2019**, *123*, 10756-10736.
72. Ruyet, R.L.; Fleutot, B.; Berthelot, R.; Benabed, Y.; Hatier, G.; Filinchuk, Y.; Janot, R. $Mg_3(BH_4)_4(NH_2)_2$ as inorganic solid electrolyte with high Mg^{2+} ionic conductivity. *ACS Appl. Energy Mater.* **2020**, *3*, 6093-6097.
73. Pang, Y.; Nie, Z.; Xu, F.; Sun, L.; Yang, J.; Sun, D.; Fang, F.; Zheng, S. Borohydride ammoniate solid electrolyte design for all-solid-state Mg batteries. *Energy Environ. Mater.* **2022**, *0*, e12527.
74. Rouhani, F.; Rafizadeh-Masuleh, F.; Morsali, A. Highly electroconductive metal-organic framework: Tunable by metal ion sorption quantity. *J. Am. Chem. Soc.* **2019**, *141(28)*, 11173-11182.
75. Yanai, N.; Uemura, T.; Horike, S.; Shimomura, S.; Kiragawa, S. Inclusion and dynamics of a polymer-Li salt complex in coordination nanochannels. *Chem. Comm.* **2011**, *47*, 1722-1724.

76. Hassan, H.K.; Farkas, A.; Varzi, A.; Jacob, T. Mixed metal-organic frameworks as efficient semi-solid electrolytes for magnesium-ion batteries. *Batteries&supecaps* **2022**, *5*, e202200260.
77. Wei, Z.; Maile, R.; Riegger, L.M.; Rohnke, M.; Muller-Buschbaum, K.; Janek, J. Ionic liquid-incorporated metal-organic framework with high magnesium ion conductivity for quasi-solid-state magnesium batteries. *Batteries&supecaps* **2022**, *5*, e202200318.
78. Zheng, Y.; Guo, J.; Ning, D.; Hunag, Y.; Lei, W.; Li, J.; Li, J.; Schuck, G.; Shen, J.; Guo, Y.; Zhang, Q.; Tian, H.; Lan, H.; Shao, H. Design of metal-organic frameworks for improving pseudo-solid-state magnesium-ion electrolytes: Open metal sites, isoreticular expansion and framework topology. *J. Mater. Sci. Tech.* **2023**, *144*, 15-27.
79. Luo, J.; Li, Y.; Zhang, H.; Wang, A.; Lo, W.-S.; Dong, Q.; Wong, N.; Povinelli, C.; Shao, Y.; Chereddy, S.; Wunder, S.; Mohanty, U.; Tsung, C.-K.; Wang, D. A metal-organic framework thin film for selective Mg^{2+} transport. *Angew. Chem. Int. Ed.* **2019**, *58*, 15313-15317.
80. Aubrey, M.L.; Ameloot, R.; Wiers, B.M.; Long, J.R. Metal-organic frameworks as solid magnesium electrolytes. *Energy Environ. Sci.* **2014**, *7*, 667-671.
81. Park, S.S.; Tukchinsky, Y.; Dinca, M. Single-ion Li^+, Na^+ and Mg^{2+} solid electrolytes supported by a mesoporous anionic Cu-azolate metal-organic framework. *J. Am. Chem. Soc.* **2017**, *139*, 13260-13263.
82. Miner, E.M.; Park, S.S.; Dinca, M. High Li^+ and Mg^{2+} conductivity in a Cu-azolate metal-organic framework. *J. Am. Chem. Soc.* **2019**, *141*, 4422-4427.
83. Yoshida, Y.; Yamada, T.; Jing, Y.; Toyao, T.; Shimizu, K.-I.; Sadakiyo, M. Super Mg^{2+} conductivity around 10^{-3} S cm^{-1} observed in a porous metal-organic framework. *J. Am. Chem. Soc.* **2022**, *144*, 8669-8675.
84. Walke, P.; Venturini, J.; Spranger, R.j.; Wullen, L.; Nilges, T. Fast Magnesium Conductiong Electrospun Solid Polymer Electrolyte. *Battery&Supercap.* **2022**, *5*, e202200285.
85. Reddy, M.J.; Chu, P.P. Ion pair formation and its effect in PEO:Mg solid polymer electrolyte system. *J. Power Sources* **2002**, *109(2)*, 340-346.
86. Basha, S.K.S.; Rao, M.C. Spectroscopic and electrochemical properties of PVP based polymer electrolyte films. *Polym. Bull.* **2018**, *75*, 3641-3666.
87. Basha, S.K.S.; Sundari, G.S.; Kumar, K.V.; Rao, M.C. Preparation and dielectric properties of PVP-based polymer electrolyte films for solid-state battery application. *Polym. Bull.* **2018**, *75*, 925-945.
88. Rathore, M.; Dalvi, A. Electrical characterization of PVA-$MgSO_4$ and PVA-Li_2SO_4 polymer salt composite electrolytes. *Mater. Today: Proceedings* **2019**, *10(1)*, 106-111.
89. Kalagi, S.S. Activation energy dependence on doping concentration in PVA-$MgCl_2$ composites. *Mater. Today: Proceedings* **2023**, 72*(5)*, 2691-2696.
90. Perumal, P.; Abhilash, K.P.; Sivaraj, P.; Selvin, P.C. Study on Mg-ion conducting solid biopolymer electrlytes based on tamarind seed polysaccharide for magnesium ion batteries. *Mater. Res. Bull.* **2019**, *118*, 110490.
91. Aziz, A.A.; Yominaga, Y. Magnesium ion-conductive polye(ethylene carbonate) electrolytes. *Ionics* **2018**, *24*, 3475-3481.
92. Aziz, A.A.; Tominaga, Y.; Effect of Li salt addition on electrochemical properties of poly(ethylene carbonate)-Mg salt electrolytes. *Polymer J.* **2019**, *51*, 61-67.
93. Viviani, M.; Meereboer, N.L.; Saeaswati, N.L.P.A.; Loos, K.; Portale, G. Lithium and magnesium polymeric electrolytes prepared using poly(glycidyl ether)-based polymers with short grafted chains. *Polym. Chem.* **2020**, *11*, 2070-2079.
94. Komal, B.; Yadav, M.; Kumar, M.; Tiwari, T.; Srivastava, N. Modifying potato starch by glutaraldehyde and $MgCl_2$ for developing an economical and environment-friendly electrolyte system. *e-Polymer* **2019**, *19*, 453-461.
95. Tamilosai, R.; Palanisamy, P.N.; Selvasekarapandian, S.; Maheshwari, T. Solium alginate incorporated with magnesium nitrate as a novel solid biopolymer electrolyte for magnesium-ion batteries. *J. Mater. Sci.:Mater. Electronics* **2021**, *32*, 22270-22285.
96. Ismayl, J.K.; Hegde, S.; Vasachar, R.; Sanjeev, G. Novel solid biopolymer electrolyte based on methyl cellulose with enhanced ion transport properties. *J. Appl. Polym. Sci.* **2022**, *139(12)*, 51826.
97. Buvaneshwari, P.; Mathavan, T.; Selvasekarapandian, S.; Krishna, M.V.; Naachiyar, R.M. Preparation and characterization of biopolymer electrolyte based on gellan gum with magnesium perchlorate for magnesium battery. Ionics **2022**, *28*, 3843-3854.
98. Rajapaksha, H.G.N.; Perera, K.S.; Vidanapathirana, K.P. Characterization of a natural rubber based solid polymer electrolyte to be used for a magnesium rechargeable cell. *Polym. Bull.* **2022**, *79*, 4879-4890.
99. Priya, S.S.; Karthika, M.; Selvasekarapandian, S.; Manjuladevi, R. Preparation and characterization of polymer electrolyte based on biopolymer I-Carrageenen with magnesium nitrate. *Solid State Ionics* **2018**, *327*, 136-149.
100. Ali, N.I.; Abidin, S.Z.Z.; Majid, S.R.; Jaafar, N.K. Role of $Mg(NO_3)_2$ as defective agent in ameliorating the electrical conductivity, structural and electrochemical properties of agarose-based polymer electrolytes. *Polymers* **2021**, *13(19)* 3357.

101. Mahalakshmi, M.; Selvanayagam, S.; Selvasekarapandian, S.; Chandra, M.V.L.; Sangeetha, P. Manjuladevi, R. Magnesium ion-conducting solid polymer electrolyte based on cellulose acetate with magnesium nitrate ($Mg(NO_3)_2$•$6H_2O$) for electrochemical studies. *Ionics* **2020**, *26*, 4553-4565.
102. Sangeetha, P.; Selvakumari, T.M.; Selvasekarapandian, S.; Srikumar, S.R.; Manjukadevi, R.; Mahalakshmi, M. Preparation and characterization of biopolymer K-carrageenan with $MgCl_2$ and its application to electrochemical devices. *Ionics* **2020**, *26*, 233-244.
103. Aziz, S.B.; Al-Zangana, S.; Woo, H.J.; Kadir, M.F.Z.; Abdullah, O.G. The compatibility of chitosan with divalent salts over monovalent salts for the preparation of solid polymer. *Results in Phys*. **2018**, *11*, 826-836.
104. Sangeetha, P.; Selvakumari, T.M.; Selvasekarapandian, S.; Mahalakshmi, M. Characterization of solid biopolymer electrolytes based on kappa-carrageenan with magnesium nitrate hexahydrate and its application to electrochemical devices. *Polymer-Plastics Tech. Mater.* **2021**, *60(12)*, 1317-1330.
105. Ismayil, J.K.; Hegde, S.; Sanjeev, G.; Murari, M.S.; An insight into the suitability of magnesium ion-conducting biodegradable methyl cellulose solid polymer electrolyte film in energy storage devices. *J. Mater. Sci.* **2023**, *58*, 5389-5412.
106. Priya, S.S.; Karthika, M.; Selvasekarapandian, S.; Manjuladevi, R.; Monisha, S. Study of biopolymer I-carrageenan with magnesium perchlorate. *Ionics* **2018**, *24*, 3861-3875.
107. Helen, P.A.; Perumal, P.; Sivaraj, P.; Diana, M.I.; Selvin, P.C. Mg-ion conducting electrolytes based on chitosan biopolymer host for the rechargeable Mg batteries. *Mater. Today: Proceedings* **2022**, *50(7)*, 2668-2670.
108. Kiruthika, S.; Malathi, M.; Selvasekarapandian, S.; Tamilarasan, K.; Moniha, V.; Manjuladevi, R. Eco-friendly biopolymer electrolyte, pectin with magnesium nitrate salt, for application in electrochemical devices. *J. Solid State Electrochem.* **2019**, *23*, 2181-2193.
109. Kiruthika, S.; Malathi, M.; Selvasekarapandian, S.; Tamilarasan, K.; Maheshwari, T. Conducting biopolymer electrolyte based on pectin with magnesium chloride salt for magnesium battery application. *Polym. Bull.* **2020**, *77*, 6299-6317.
110. Kayama, N.; Homma, K.; Yamakawa, Y.; Hirayama, M.; Kanno, R.; Yoneyama, M.; Kamiyama, T.; Kato, Y.; Hama, S.; Kawamoto, K.; Mitsui, A. A lithium superionic conductor, *Nat. Mater.* **2011**, *10(9)*, 682-686.
111. Rathika, R.; Suthanthiraraj, S.A. Ionic interactions and dielectric relaxation of PEO/PVDF-Mg[$(CF_3SO_2)_2N_2$] blend electrolytes for magnesium ion rechargeable batteries. *Macromolecular Res.* **2016**, *24*, 422-428.
112. Shenbagavalli, S.; Muthuvinayagam, M.; Revathy, M.S. Electrical properties of Mg^{2+} ion-conductive PEO:P(PVdF-HFP) based solid blend polymer electrolytes. *Polymer* **2022**, *256*, 125242.
113. Manjuladevi, R.; Thamilselvan, M.; Selvasekarapandian, S.; Mangalam, R.; Premalatha, M.; Monisha, S. Mg-ion conducting blend polymer electrolyte based on poly(vinyl alcohol)-poly(acrylonitrile) with magnesium perchlorate. *Solid State Ionics* **2017**, *308*, 90-100.
114. Ponmani, S.; Prabhu, M.R. Development and study of solid polymer electrolytes based on PVdF-HFP/PVAc:$Mg(ClO_4)_2$ for Mg ion batteries. *J. Mater. Sci.: Mater. Electronics* **2018**, *29*, 15086-15096.
115. Polu, A.R.; Kumar, R.; Rhee, H.-W. Magnesium ion conducting solid polymer blend electrolyte based on biodegradable polymers and application in solid-state batteries. *Ionics* **2015**, *21*, 125-132.
116. Manjuladevi, R.; Thamilselvan, M.; Selavasekarapandian, S.; Selvin, P.C.; Mangalam, R.; Monisha, S. Preparation and characterization of blend polymer electrolyte film based on poly(vinyl alcohol)-poly(aceylonitrile)/$MgCl_2$ for energy storage devices. *Ionics* **2018**, *24*, 1083-1095.
117. Ponraj, T.; Ramalingam, A.; Selvasekarapandian, S.; Srikumar, S.R.; Manjuladevi, R. Mg-ion conducting triblock copolymer electrolyte based on poly(VdCl-co-AN-co-MMA) with magnesium nitrate. *Ionics* **2020**, *26*, 789-800.
118. Hiraoka, K.; Inoue, M.; Takahashi, K.; Hayamizu, K.; Watanabe, M.; Seki, S. Analysis of ionic transport and electrode interfacial reaction, and NMR one-dimensional imaging of ther-based polymer electrolytes. *J. Electrochem. Soc.* **2021**, *168(6)*, 060501.
119. Park, B.; Andersson, R.; Pate, S.G.; Liu, J.; O'brien, C.P.; Hernandez, G.; Mindemark, J.; Schaefer, J.L. Ion coordination and transport in magnesium polymer electrolytes based on polyester-co-polycarbonate. *Energy Mater. Adv.* **2021**, 9895403.
120. Manjuladevi, R.; Selvasekarapandian, S.; Thamilselvan, M.; Mangalam, R.; Monisha, S.; Selvin, P.C. A study on blend polymwe electrolyte based on poly(vinyl alcohol)-poly(acrylonitrile) with magnesium nitrate for magnesium battery. *Ionics* **2018**, *24*, 3493-3506.
121. Ponmani, S.; Kalaiselvimary, J.; Prabhu, M.R. Structural, electrical, and electrochemical properties of poly(vinylidene fluoride-co-hexaflouropropylene)/poly(vinyl acetate)-based polymer blend electrolytes for rechargeable magnesium ion batteries. *J. Solid State Electrochem.* **2018**, *22*, 2605-2615.
122. Nayak, P.; Ismayil; Cyriac, V.; Hegde, S.; Sanjeev, G.; Murari, M.S.; Sudhakar, Y.N. Magnesium ion conducting free-standing biopolymer blend electrolyte films for electrochemical device application. *J. Non-crystalline Solids* **2022**, *592*, 121741.
123. Suvarnna, K.; Kirubavathy, S.J.; Selvasekarapandian, S.; Krishna, M.V.; Ramaswamy, M. Corn silk extract-based solid-state biopolymer electrolyte and its application to electrochemical storage devices. *Ionics* **2022**, *28*, 1767-1782.

124. Kanakaraj, T.M.; Bhajantri, R.F.; Chavan, C.; Cyriac, V.; Bulla, S.S.; Ismayil. Investigation on the structural and ion transport properties of magnesium salt doped HPMC-PVA based polymer blend for energy storage applications. *J. Non-crystalline Solids* **2023**, 603, 122276.
125. Koduru, H.K.; Marinov, Y.G.; Kaleemulla, S.; Rafailov, P.M.; Hadjichristov, G.B.; Scaramuzza, N. Fabrication and characterization of magnesium-ion-conducting flexible polymer electrolyte membranes based on a nanocomposite of poly(ethylene oxide) and potate starch nanocrystals. *J. Solid State Electrochem.* **2021**, 25, 2409-2428.
126. Kotobuki, M.; Kanamura, K. Fabrication of all-solid-state battery using $Li_5La_3Ta_2O_{12}$ Ceramic electrolyte. *Ceram. Int.* **2013**, *39(6)*, 6481-6487.
127. Sarangika, H.N.M.; Dissanayake, M.A.K.L.; Senadeera, G.K.R.; Rathnayake, R.R.D.V.; Pitawala, H.M.J.C. Polyethylene oxide and ionic liquid-based solid polymer electrolyte for rechargeable magnesium batteries. *Ionics*, **2017**, *23*, 2829-2835.
128. Ge, X.; Song, F.; Du, A.; Zhang, Y.; Xie, B.; Huang, L.; Zhao, J.; Dong, S.; Zhou, X.; Cui, G. Robust self-standing single-ion polymer electrolytes enabling high-safety magnesium batteries at elevated temperature. *Adv. Energy Mater.*, **2022**, *12(31)*, 2201464.
129. Gupta, A.; Jain, A.; Tripathi, S.K. Structural and electrochemical studies of bromide derived ionic liquid-based gel polymer electrolyte for energy storage. *J. Energy Storage*, **2020**, *32*, 101723.
130. Hambali, D.; Zainol, N.H.; Othman, L.; Isa, K.B.M.; Osman, Z. Magnesium ion-conducting gel polymer electrolytes based on poly(vinylidene chloride-co-acrylonitrile) (PVdC-co-AN): a comparative study between magnesium trifluoromethanesulfonate ($MgTf_2$) and magnesium bis(trifluoromethanesulfonimide) ($Mg(TFSI)_2$). *Ionics*, **2019**, *25*, 1187-1198.
131. Maheshwaran, C.; Mishra, K.; Kanchan, D.K.; Kumar, D. Mg^{2+} conducting polymer gel electrolytes: physical and electrochemical investigations. *Ionics*, **2020**, *26*, 2969-2980.
132. Kotobuki, M.; Yan, B.; Lu, L. Recent progress on cathode materials for rechargeable magnesium batteries. *Energy storage Mater.* **2023**, *54*, 227-253.
133. Doe, R.E.; Han, R.; Hwang, J.; Gmitter, A.J.; Shterenberg, I.; Yoo, H.D.; Pour, N.; Aurbach, D. Novel electrolyte solutions comprisingly fully inorganic salts with high anodic stability for rechargeable magnesium batteries. *Chem. Comm.*, **2014**, *50*, 243-245.
134. Wang, T.; Zhao, X.; Liu, F.; Fan, L.-Z. Porous polymer electrolytes for long-cycle stable quasi-solid-state magnesium batteries. *J. Energy Chem.*, **2021**, *59*, 608-614.
135. Merrill, L.C.; Ford, H.O.; Scaefer, J.L. Application of single-ion conducting gel polymer electrolytes in magnesium batteries. *ACS Appl. Energy Mater.*, **2019**, *2*, 6355-6363.
136. Sheha, E.; Liu, F.; Wang, T.; Farrag, M.; Liu, J.; Yacout, N.; Kebebe, M.A.; Sharma, N.; Fan, L.-Z. Dual polymer/liquid electrolyte with $BaTiO_3$ electrode for magnesium batteries. *ACS Appl. Energy Mater.*, **2020**, *3*, 5882-5892.
137. Maheshwaran, C.; Kanchan, D.K.; Gohel, K.; Mishra, K.; Kumar, D. Effect of $Mg(CF_3SO_3)_2$ concentration on structural and electrochemical properties of ionic liquid incorporated polymer electrolyte membranes. *J. Solid State Electrochem.*, **2020**, *24*, 655-665.
138. Hambali, D.; Osman, Z.; Othman, L.;Isa, K.B.M.; Harudin, N. Magnesium (II) bis(trifluoromethanesulfonimide) doped PVdC-co-AN gel polymer electrolytes for rechargeable batteries. *J. Polym. Res.*, **2020**, *27*, 159.
139. Gupta, A.; Jain, A.; Tripathi, S.K. Structural, electrical and electrochemical studies of ionic liquid-based polymer gel electrolyte using magnesium salt for supercapacitor application. *J. Polym. Res.*, **2021**, *28*, 235.
140. Aziz, A.; Yoshimoto, N.; Yamabuki, K.; Tominaga, Y. Ion-conductive, thermal and electrochemical properties of poly(ethylene carbonate)-Mg electrolytes with glyme solution. *Chem. Lett.*, **2018**, *47*, 1258-1261.
141. Sharma, J.; Hashmi, S.A. Plastic crystal-incorporated magnesium ion conducting gel polymer electrolyte for battery application. *Bull. Mater. Sci.*, **2018**, *41*, 147.
142. Ponraj, T.; Tamalingam, A.; Selvasekarapandian, S.; Srikumar, S.R.; Manjuladevi, R. Plasticized solid polymer electrolyte based on triblock copolymer polyvinylidene chloride-co-acrylonitrile-co-methyl methacrylate for magnesium ion batteries. *Polym. Bull.*, **2021**, *78*, 35-57.
143. Tominaga, Y.; Kato, S.; Nishimura, N. Preparation and electrochemical characterization of magnesium gel electrolytes based on crosslinked poly(tetrahydrofuran). *Polymer*, **2021**, *224*, 123743.
144. Hamsan, M.H.; Aziz, S.B.; Kadir, M.F.Z.; Brza, M.A.; Karim, W.O. The study of EDLC device fabricated from plasticized magnesium ion conducting chitosan based polymer electrolyte. *Polym. Testing*, **2020**, *90*, 106714.
145. Sangeetha, P.; Selvakumari, T.M.; Selvasekarapandian, S.; Mahalakshmi, M. Characterization of solid biopolymer electrolytes based on kappa-carrageenan with Magnesium nitrate hexahydrate and its application to electrochemical devices. *Polym.-Plastic Tech. Mater.* **2021**, *60(12)*, 1317-1330.
146. Ponmami, S.; Prabhu, M.R. Sulfonate based ionic liquid incorporated polymer electrolytes for Magnesium secondary battery. *Polym.-Plastic Tech. Eng.*, **2019**, *58(9)*, 978-991.

147. Nishino, H.; Liu, C.; Kanehashi, S.; Mayumi, K.; Tominaga, Y.; Shimomura, T.; Ito, K. Ionics transport and mechanical properties of slide-ring gel swollen with Mg-ion electrolytes. *Ionics*, **2020**, *26*, 255-261.
148. Singh, R.; Janakiraman, S.; Khalifa, M.; Anandhan, S.; Ghosh, S.; Venimadhav, A.; Biswas, K. An electroactive β-phase polyvinylidene fluoride as gel polymer electrolyte for magnesium-ion battery application. *J. Electroanal. Chem.*, **2019**, *851*, 113417.
149. Bhatt, P.J.; Pathak, N.; Mishra, K.; Kanchan, D.K.; Kumar, D. Effect of different cations on ion-transport behavior in polymer gel electrolytes intended for application in flexible electrochemical devices. *J. Electronic Mater.*, **2022**, *51*, 1371-1384.
150. Wang, L.; Li, Z.; Meng, Z.; Xiu, Y.; Dasari, B.; Zhao-Karger, Z.; Fichtner, M. Designing gel polymer electrolytes with synergetic properties for rechargeable magnesium batteries. *Energy Storage Mater.*, **2022**, *48*, 155-163.
151. Wang, J.; Zhao, Z.; Muchakayala, R.; Song, S. High-performance Mg-ion conducting poly(vinyl alcohol) membranes: Preparation, characterization and application in supercapacitors. *J. Membrane Sci.*, **2018**, *555*, 280-289.
152. Singh, R.; Janakiraman, S.; Agrawal, A.; Ghosh, S.; Venimadhav, A.; Biswas, K. An amorphous poly(vinylidene fluoride-co-hexafluoropropylene) based gel polymer electrolyte for magnesium ion battery. *J. Electroanal. Chem.*, **2020**, *858*, 113788.
153. Singh, R.; Janakiraman, S.; Khalifa, M.; Anandhan, S.; Ghosh, S.; Venimadhav, A.; Biswas, K. A high thermally stable polyacrylonitrile (PAN)-based gel polymer electrolyte for rechargeable Mg-ion battery. *J. Mater. Sci.: Mater. Electron*, **2020**, *31*, 22912-22925.
154. Maheshwaran, C.; Kanchan, D.K.; Mishra, K.; Kumar, D.; Gohel, K. Flexible, magnesium-ion conducting polymer electrolyte membrane: mechanical, structural, thermal, and electrochemical impedance spectroscopic properties. *J. Mater. Sci.: Mater. In Electronics*, **2020**, *31*, 15013-15027.
155. Abdulwahid, R.T.; Aziz, S.B.; Brza, M.A.; Kadir, M.F.Z.; Karim, W.O.; Hamsan, H.M.; Asnawi, A.S.F.M.; Abdullah, R.M.; Nofal, M.M.; Dannoun, E.M.A. Electrochemical performance of polymer blend electrolytes based on chitosan: dextran: impedance, dielectric properties, and energy storage study. *J. Mater. Sci.: Mater. Electron*, **2021**, *32*, 14846-14862.
156. Ota, T.; Uchiyama, S.; Tsukada, K.; Moriya, M. Room-temperature Mg-ion conduction through molecular crystal $Mg\{N(SO_2CF_3)_2\}_2(CH_3OC_5H_9)_2$. *Front. Energy Res.*, **2021**, *9*, 640777.
157. Mori, S.; Obora, T.; Namaki, M.; Kondo, M.; Moriya, M. Organic crystalline solid electrolytes with high Mg-ion conductivity composed of nonflammable ionic liquid analogs and $Mg(TFSA)_2$. *Inorg. Chem.*, **2022**, *61*, 7358-7364.
158. Jayanthi, S.; Kalapriya, K. Structural, transport, morphological, and thermal studies of nano barium titanate-incorporated magnesium ion conducting solid polymer electrolytes. *Polym. Polym. Composites*, **2021**, *29*, S1158-S1167.
159. Wang, Y.; Wang, Z.; Zheng, F.; Sun, J.; Oh, J.A.S.; WU, T.; Chen, G.; Huang, Q.; Kotobuki, M.; Lu, L. Ferroelectric engineered electrode-composite polymer electrolyte interfaces for all-solid-state sodium metal battery. *Adv. Sci.*, **2022**, *9(13)*, 2105849.
160. Jeyabanu, K.; Sundaramahalingam, K.; Devendran, P.; Manikandan, A.; Nallamuthu, N. Effect of electrical conductivity studied for CuS nanofillers mixed magnesium ion based PVA-PVP blend polymer solid electrolytes. *Phys. B: Condenced Matter*, **2019**, *572*, 129-138.
161. Jayalakshmi, K.; Ismayil,; Hedge, S.; Ravindrachary, V.; Sanjeev, G.; Mazumdar, N.; Sindhoora, K.M.; Masti, S.P.; Murari, M.S. Methyl cellulose-based solid polymer electrolytes with dispersed zinc oxide nanoparticles: A promising candidate for battery applications. *J. Phys. Chem. Solids*, **2023**, *173*, 111119.
162. Nidhi, Patel, S.; Kumar, R. Synthesis and characterization of magnesium ion conductive in PVDF based nanocomposite polymer electrolytes disperse with MgO. *J. Alloy Compd.*, **2019**, *789*, 6-14.
163. Polu, A.; Kumar, R. Preparation and characterization of PEG-Mg(CH3COO)2-CeO2 composite polymer electrolytes for battery application. *Bull. Mater. Sci.*, **2014**, *37(2)*, 309-314.
164. Sarojini, S.; Padmapriya, L. Effect of size of the filler on the electrical conductivity of magnesium ion conducting polymer electrolyte. *Mater. Today: Proceedings*, **2022**, *68*, 454-462.
165. Helen, P.A.; Selvin, P.C.; Lashmi, D.; Diana, M.I. Amelioration of ionic conductivity (303K) with the supplement of MnO_2 filler in the chitosan biopolymer electrolyte for magnesium batteries. *Polym. Bull.*, **2023**, *80*, 7715-7740.
166. Maheshwaran, C.; Kanchan, D.K.; Mishra, K.; Kumar, D.; Gohel, K. Effect of active MgO nano-particles dispersion in small amount within magnesium-ion conducting polymer electrolyte matrix. *Nano-structures&nano-objects*, **2020**, *24*, 100587.
167. Nidhi, Patel, S.; Kumar, R. Effect of Al_2O_3 on electrical properties of polymer electrolyte for electrochemical device application. *Mater. Today: Proceedings*, **2021**, *46*, 2175-2178.
168. Nidhi, Patel, S.; Kumar, R. Effect of nanoparticles on electrical properties of PVDF-based Mg^{2+} ion conducting polymer electrolytes. *Bull. Mater. Sci.*, **2021**, *44*, 140.

169. Sundar, M.; Selladurai, S. Effect of fillers on magnesium-poly(ethylene oxide) solid polymer electrolyte. *Ionics*, **2006**, *12*, 281-286.
170. Ponmani, S.; Selvakumar, K.; Prabhu, M.R. The effect of the geikeilite ($MgTiO_3$) nanofiller concentration in PVdF-HFP/PVAc-based polymer blend electrolytes for magnesium ion battery. *Ionics*, **2020**, *26*, 2353-2369.
171. Helen, P.A.; Ajith, K.; Diana, M.I.; Lakshmi, D.; Selvin, P.C. Chitosan based biopolymer electrolyte reinforced with V_2O_5 filler for magnesium batteries: an inclusive investigation. *J. Mater. Sci.: Mater. Electron*, **2022**, *33*, 3925-3937.
172. Mallikarjun, A.; Sangeetha, M.; Mettu, M.R.; Reddy, J.M.; Kumar, S.J.; Sreekanth, T.; Rao, V.S. Impedance spectroscopy and electrochemical cell studies of Mg^{2+} ion conducting with dispersed ZrO_2 nano filler in PVDF-HFP based nano composite solid polymer electrolytes. *Mater. Today: Proceedings*, **2022**, *62*, 5204-5208.
173. Patel, N.S.; Kumar, R. PVDF-HFP based nanocomposite polymer electrolytes for energy storage devices dispersed with various nano-fillers. *AIP Conference Proceedings*, **2020**, *2220*, 080044.
174. Dannoun, E.M.A.; Aziz, S.B.; Brza, M.A.; Nofal, M.M.; Asnawi, A.S.F.M.; Yusof, Y.M.; Al-Zangana, S.; Hamsan, M.H.; Kadir, M.F.Z.; Woo, H.J. The study of plasticized solid polymer blend electrolytes based on natural polymers and their application for energy storage EDLC devices. *Polymers*, **2020**, *12(11)*, 2531.
175. Song, S.; Kotobuki, M.; Zheng, F.; Li, Q.; Xu, C.; Wang, Y.; Li, W.D.Z.; Hu, N.; Lu, L. Communication-A composite polymer electrolyte for safer Mg batteries. *J. Electrochem. Soc.*, **2017**, *164(4)*, A741-A743.
176. Aziz, S.B.; Dannoun, E.M.A.; Hamsan, M.H.; Abdulwahid, R.T.; Mishra, K.; Nofal, M.M.; Kadir, M.F.Z. Improving EDLC device performance constructed from plasticized magnesium ion conducting chitosan based polymer electrolytes via metal complex dispersion. *Membranes*, **2021**, *11(4)*, 289.
177. Sharma, J.; Hashmi, S. Magnesium ion-conducting gel polymer electrolyte nanocomposites: Effect of active and passive nanofillers. *Polym. Composites*, **2019**, *40(4)*, 1295-1306.
178. Deivanayagam, R.; Cheng, M.; Wang, M.; Vasudevan, V.; Foroozan, T.; Medhekar, N.V.; Shahbazian-Yassar, R. Composite polymer electrolyte for highly cyclable room-temperature solid-state magnesium batteries. *ACS Appl. Energy Mater.*, **2019**, *2*, 7980-7990.
179. Sun, J.; Zou, Y.; Gao, S.; Shao, L.; Chen, C. Robust strategy of quasi-solid-state electrolytes to boost the stability and compatibility of Mg ion batteries. *ACS Appl. Mater. Interfaces*, **2020**, *12*, 54711-54719.
180. Wang, P.; Truck, J.; Hacker, J.; Schlosser, A.; Kuster, K.; Starke, U.; Reinders, L.; Buchmeiser, M.R. A design concept for halogen-free Mg^{2+}/Li^+-dual salt-containing gel-polymer-electrolytes for rechargeable magnesium batteries. *Energy Storage Mater.*, **2022**, *49*, 509-517.
181. Luo, W.; Allen, M.; Raji, V.; Ji, X. An organic pigment as a high-performance cathode for sodium-ion batteries. *Adv. Energy Mater.* **2014**, *4(15)*, 1400554.
182. Chen, Y.; Luo, W.; Cater, M.; Zhou, L.; Dai, J.; Fu, K.; Lacey, S.; Li, T.; Wan, J.; Han, J.; Bao, Y.; Hu, L. Organic electrode for non-aqueous potassium-ion batteries. *Nano Energy*, **2015**, *18*, 205-211.
183. Chen, Y.; Parent, L.R.; Shao, Y.; Wang, C.; Sprenkle, V.L.; Li, G.; Liu, J. Facile synthesis of chevrel phase nanocubes and their applications for multivalent energy storage. *Chem. Mater.* **2014**, *26*, 4904-4907.
184. Mao, M.; Lin, Z.; Tong, Y.; Yue, J.; Zhao, C.; Lu, J.; Zhang, Q.; Gu, L.; Suo, L.; Hu, Y.S.; Li, H.; Huang, X.; Chen, L. Iodine vapor transport-triggered preferential growth of chevrel Mo_6S_8 nanosheets for advanced multivalent batteries. *ACS Nano*, **2020**, *14*, 1102-1110.